Flow sensing in the deep sea: the lateral line system of stomiiform fishes

ASHLEY N. MARRANZINO[1] and JACQUELINE F. WEBB[1,2*]

¹Department of Biological Sciences, University of Rhode Island, 120 Flagg Road, Kingston, RI 02881, USA
²Associate of Ichthyology, Museum of Comparative Zoology, Harvard University, 26 Oxford St., Cambridge, MA 02138, USA

Fishes inhabiting the deep sea are notable for the production of bioluminescence and specializations of their visual systems. However, they are also equipped with non-visual sensory systems that probably mediate critical behaviours as they do in other fishes, but they are not well-studied. The mechanosensory lateral line system of fishes in the order Stomiiformes, the largest and most diverse order of deep-sea fishes, was studied in detail in 28 species (in 17 of 52 genera, in all four stomiiform families) using several morphological methods. Some or all of the narrow cranial lateral line canals are partially reduced or absent in representatives of all genera examined. In addition, hundreds to thousands of small superficial neuromasts were found on the head and body in 17 species in 11 genera of sternoptychids, gonostomatids and stomiids. Reported here for the first time, this feature of the lateral line system would enhance sensitivity to the velocity component of water flows (probably of biotic origin) and is hypothesized to be an adaptation in the low-light environment of the deep sea. These observations require that we think beyond vision when considering the behaviour and sensory ecology of these critically important and globally distributed deep-sea fishes.

ADDITIONAL KEYWORDS: µCT – bathypelagic – mechanosensory – mesopelagic – neuromast – osteology – receptor organ – sensory.

INTRODUCTION

The sensory environment of the deep sea presents challenges to fishes whose survival and fitness depend on the ability to navigate a featureless 3D environment, detect and avoid predators, find and capture food and successfully reproduce. Life in these dimly lit waters has favoured the evolution of bioluminescence and some remarkable visual adaptations (Douglas & Partridge, 2011; Gagnon, Sutton & Johnsen, 2013; Davis *et al.*, 2014; De Busserolles, Marshall & Collin, 2014). Substantially less is known about the non-visual sensory systems (olfaction, taste, hearing, mechanoreception) of deep-sea fishes, but it is likely that it is the integration of input from multiple sensory modalities that is important for mediating behaviours, as is the case in other fishes (e.g. Butler & Maruska, 2016).

The mechanosensory lateral line system detects unidirectional water flows and low frequency vibrations at short range (up to a few body lengths) and mediates prey detection, predator avoidance, navigation and communication (Montgomery, Bleckmann & Coombs, 2014; Webb, 2014b; Butler & Maruska, 2016). In bony fishes, the neuromast receptor organs of the lateral line system are located on the skin of the head, trunk, and tail (superficial neuromasts [SNs]) and within pored canals (canal neuromasts) located in a subset of skull bones and in the lateral line scales on the trunk (Webb, 2014a, b). They are composed of mechanosensory hair cells (like those in the inner ear), which are directionally sensitive to water flows. Furthermore, the location of the neuromasts (in canals or on the skin) defines two sub-modalities that respond to two distinct physical components of water flows – canal neuromasts, which detect flow acceleration and SNs, which detect flow velocity (Denton & Gray, 1989; McHenry & Liao, 2014). Enhanced sensitivity of the lateral line system would allow fishes to respond more

---

*Corresponding author. E-mail: jacqueline_webb@uri.edu

effectively to hydrodynamic stimuli (from biotic and abiotic sources), especially in those habitats or situations in which fish experience low levels of background hydrodynamic noise (e.g. little turbulence or localized vibrations and flows), including the deep sea.

Five cranial lateral line canal phenotypes are found among bony fishes – narrow (simple, with widened tubules or with branched tubules), widened and reduced canals (reviewed in Webb, 2014b). Two of these are of particular interest as adaptations for enhancement of sensitivity to hydrodynamic stimuli: widened canals, which have large canal pores and large canal neuromasts (e.g. Eurasian Ruffe, *Gymnocephalus cernuus*), and reduced canals, which are typically accompanied by a proliferation of small SNs that are found in discrete linear series or are scattered over the skin on the head and/or trunk [e.g. gobies (family Gobiidae)]. In freshwater fishes, each of these phenotypes has evolved convergently among nocturnal fishes, those that live in dimly lit waters at considerable depths in lakes and rivers, and in eyeless cave-dwelling fishes (e.g. Mexican blind cavefish, *Astyanax mexicanus*, Yoshizawa *et al.*, 2010; Yamamoto & Jeffery, 2011; cichlids, Schwalbe, Bassett & Webb, 2012; reviewed in Webb, 2014b).

Widened lateral line canals and reduced canals with SN proliferations are also found in taxa inhabiting the deep sea (reviewed in Webb, 2014b). Widened canals are found in deep-sea species in the Stephanoberyciformes (Marshall, 1996), Gadiformes (Marshall, 1965; Fange, Larsson & Lidman, 1972), Ophidiiformes (Jakubowski, 1974; Marshall, 1996), Lophiiformes (Caruso, 1989; Marshall, 1996) and Trachichthyiformes (Jakubowski, 1974; Moore, 1993). Reduced canals accompanied by a proliferation of SNs (typically located on raised papillae) are found among deep-sea fishes in the Anguilliformes (Mead & Rubinoff, 1966), Saccopharyngiformes (Nielsen & Bertelsen, 1985) and Lophiiformes (Marshall, 1996). In other deep-sea taxa, a proliferation of SNs is reported to accompany either well-developed narrow or widened canals (in some members of Halosauridae, Melamphaidae, Searsiidae, Myctophidae, Evermannellidae, Ipnopidae, Macrouridae, Cetomimiformes; Marshall, 1954, 1979; Theisen, 1959; Lawry, 1972a, b; Marshall & Staiger, 1975; Caruso, 1989; Harold, 2002).

The order Stomiiformes is the most speciose group of deep-sea fishes (with ~412 spp. in 52 genera; Nelson, Grande & Wilson, 2016), but little is known about their lateral line system. The order is composed of four families: Sternoptychidae (hatchetfishes; 73 species in ten genera), Gonostomatidae (bristlemouths; 31 species in eight genera), Phosichthyidae (24 species in seven genera) and the Stomiidae (barbeled dragonfishes; ~286 species in 27 genera; Nelson *et al.*, 2016). These fishes

are major components of the deep scattering layer and deep-sea food webs (Bigelow *et al.*, 1964; Maynard, 1982; Sutton & Hopkins, 1996). They are commonly collected and archived as museum specimens, yet only incidental observations about, or indirect references to, their lateral line system are found in the literature (Weitzman, 1967, 1974; Marshall, 1979; Maynard, 1982; Fink, 1985). In the only published article that has directly addressed the morphology of the lateral line system of stomiiforms, Handrick (1901) reported that the hatchetfish, *Argyropelecus hemigymnus* Cocco, 1829, has reduced cranial lateral line canals and a small number of SNs (a total of 27 neuromasts). This is at odds with reports of substantially higher numbers of SNs in other deep-sea taxa and is contrary to the prediction that fishes in the light-limited deep sea should have a more sensitive mechanosensory lateral line system. Thus, the goal of this study was to examine the lateral line system in *Argyropelecus* spp. and in representative taxa in all four families of the order Stomiiformes to better understand the sensory biology of this important group.

MATERIAL AND METHODS

Study material was obtained from the ichthyology collection of the Museum of Comparative Zoology (MCZ, Harvard University) or was collected at sea (Appendix 1). Specimens were fixed in 10% formalin (typically in seawater) in which they were stored or later transferred to 70% ethanol for long-term storage (Appendix 1). A combination of morphological methods was used to describe cranial lateral line canal and neuromast morphology and distribution in 28 representative species in 17 of 52 genera belonging to all four families in the order Stomiiformes. The study focused on only those specimens that were determined to be in good enough condition for analysis, which resulted in a detailed treatment of a relatively small number of specimens in each species.

All specimens were imaged using a dissecting microscope (Nikon SMZ1500 with SPOT RT3 25.2 2 MP colour mosaic camera) and SPOT 5.2 imaging software (Diagnostic Instruments, Inc.). Images in multiple planes of focus were combined into a single image using Helicon Focus (Helicon Soft Ltd.). Imaging revealed the presence/absence of canal pores in the epithelium, indicative of the presence of cranial lateral line canals and locations of SNs.

Other specimens were enzymatically cleared and stained for bone and cartilage (Pothoff, 1984) or imaged using micro-computed tomography (µCT). All µCT data were generated using a Bruker SkyScan 1173 (at the Museum of Comparative Zoology, Harvard University) with a resolution of 14.9–54.7 µm. The

presence or absence of cranial lateral line canals was confirmed by examining 2D slices. 3D data were reconstructed using the volume rendering protocol in OsiriX (v3.6.1, 64 bit).

Variation in canal morphology along the length of a canal, among canals in an individual and among taxa was reminiscent of the stages of development of the lateral line canals described in other teleost taxa (Tarby & Webb, 2003; Webb & Shirey, 2003; Bird & Webb, 2014). Briefly, presumptive canal neuromasts differentiate in the epidermis (Stage 1) and each sinks into a depression (Stage 2a). Then, canal walls grow up on either side of the neuromast within the dermis (Stage 2b) forming a partially developed canal segment, and the walls associated with adjacent neuromasts may form a continuous trough. The soft tissue covering the canal walls fuses over the neuromast providing a soft tissue covering for the canal (Stage 3). The canal walls then grow within the soft tissue fusing over the neuromast to form an ossified canal segment (Stage 4). Finally, adjacent canal segments fuse, forming a fully ossified canal leaving bony canal pores between neuromast positions. Thus, these stages of development were used in describing variation in canal morphology in adult stomiiforms (see Table 1). The presence of a canal was indicated by the presence of an open trough in a bone (an incompletely ossified canal, which may be covered by soft tissue) or by bony canal pores (indicating an

Table 1. Morphology of lateral line canals (as defined by developmental stages 1–4, Bird & Webb, 2014) determined through study of whole preserved specimens, histology and μCT imaging

Family	Species	Canals				
		SO	MD	PO	IO	Other
Sternoptychidae	*Argyropelecus aculeatus*	3–4	3	3	0	0
	A. affinis	3–4	3	3	0	0
	A. hemigymnus	3–4	3	3	0	0
	A. lychnus	3–4	3	3	0	0
Gonostomatidae	*Cyclothone acclinidens*	0	0	0	0	0
	C. alba	0	0	0	0	0
	C. braueri	0	0	0	0	0
	C. microdon	0	0	0	0	0
	C. parapallida	0	0	0	0	0
	C. pallida	0	0	0	0	0
	C. pseudopallida	0	0	0	0	0
	C. signata	0	0	0	0	0
	Gonostoma elongatum	3	0	3	3/4	3/4–4
Stomiidae	*Aristostomias tittmanni*	4	4–2b/3	4	–	–
	Astronesthes niger	4	4–3	4–3	3	4–3/4
	A. gemmifer	4	4–3	4–2b/3	-	4–3/4
	Bathophilus filifer	3/4	3/4	3/4	0	3/4
	Echiostoma barbatum	3–4	4–3	4–3	0	3
	Eustomias hulleyi	3/4	3/4	3/4	0	3/4
	Flagellostomias boureei	3/4	3/4	3/4	3/4	3/4
	Idiacanthus antrostomus	3/4	3/4	0	3/4	3/4
	Malacosteus niger	4	2b/3	2b/3	–	–
	Neonesthes capensis	4	4–2b/3	4	–	2b/3
	Opostomias micripnus	3/4	3/4	3/4	3/4	3/4
	Pachystomias sp.	2b/3–4	2b/3	4–2b/3	–	4
	Rhadinesthes decimus	4	4	4–2b/3	–	–
	Tactostoma macropus	3/4	3/4	3/4	3/4	3/4
Phosichthyidae	*Ichthyococcus ovatus*	–	4	4–2b/3	–	–

Canals are supraorbital (SO), mandibular (MD), preopercular (PO), infraorbital (IO) and other canals (including the otic, post-temporal and/or supratemporal commissure). Degree of canal ossification is based on the developmental stages (St. 1–4; defined in Bird & Webb, 2014). '4' = fully enclosed and ossified canal; '3/4' = fully enclosed, but degree of ossification unclear (determined in whole specimens only); '3' = fully enclosed, partially ossified canal; '2b/3' = partially ossified, and either open or enclosed, respectively (defined by bony trough in μCT reconstructions); '0' = canal absent; '–' = no data or unable to determine. A range of stages is noted in rostro-caudal sequence (SO, MD, other canals) or in ventral-dorsal sequence (PO canal) where the degree of ossification varies within a canal. See text for additional information. Size, number of specimens and method of examination are found in Appendix 1.

enclosed and fully ossified canal). Finally, the presence of epithelial canal pores (perforations in the skin) in whole preserved specimens was indicative of the presence of an enclosed or ossified canal.

Histological material was used to further characterize the morphology of the canals and of both canal and SNs. Specimens were decalcified in Cal-Ex (Thermo Fisher Scientific) for 2 h, dehydrated in ascending concentrations of ethanol and t-butyl alcohol, embedded in Paraplast (Thermo Fisher Scientific), serially sectioned (8 µm thickness, transverse sections) and mounted on slides subbed with 10% albumin in 0.9% NaCl. Sections were stained (Hall and Burnt Quadruple stain; Hall, 1986) and coverslipped (Entellan, Electron Microscopy Sciences). Other specimens (or portions of specimens) were embedded in glycol methacrylate plastic resin (Technovit 7100, Electron Microscopy Sciences) and sectioned transversely at 5 µm on a Leica 4M2265 microtome. Every third section was mounted out of dH$_2$O onto clean slides, dried on a slide warmer overnight, stained with 0.5% aqueous cresyl violet (5 min, followed by 1- to 2-min tap water rinse), air-dried overnight and coverslipped with Entellan (Electron Microscopy Sciences).

Scanning electron microscopy (SEM) was used to further verify SN identity, morphology and orientation (axis of best physiological sensitivity) in *Argyropelecus*, *Cyclothone* and *Bathophilus* (methods in Webb & Shirey, 2003; Bird & Webb, 2014). Specimens were viewed at a voltage of 3 kV and a working distance of ~10 mm on a Zeiss NTS Supra 40VP SEM.

Additional whole preserved *Argyropelecus* spp. and *Cyclothone* spp. were bleached in 3% H$_2$O$_2$ in 1% KOH for 30–90 min depending on the degree of pigmentation present. Specimens were subsequently stained with Meyer's haematoxylin (Sigma). Staining times ranged from 1 to 45 min (dependent on the specimen and haematoxylin solution used); specimens were removed from the haematoxylin and viewed to determine whether SNs were stained sufficiently to be differentiated from the general epithelium.

It should be noted that specimen condition was critical for an assessment of neuromast number and distribution. Examination of specimens and histological material prepared (as above) revealed that the epithelium is only a few cell layers thick and quite susceptible to damage. Even those specimens appearing to be in excellent condition had some skin damage upon closer examination. In cases where the thin epithelium was abraded, small depressions underlain by pigment were found in the skin in the same locations as small SNs in specimens of the same or related species. For example, SEM revealed that the majority of these depressions in a specimen of *Bathophilus* was covered by debris, but others were clean and lined by a smooth cell layer that lacked the microridges and

cellular boundaries characteristic of the intact skin surface of other fishes (data not shown). Thus, these depressions were interpreted as the locations of neuromasts in the epidermis that had been damaged during collection, handling and storage. Inclusion of both neuromasts and these small depressions provides a more accurate assessment of SN number in some species. In the descriptions provided below, neuromast counts are given for one side of the head and body (e.g. in lateral view), unless otherwise noted.

RESULTS

All taxa examined have reduced canals (defined by Webb, 2014b), with at least some canals that are only partially ossified or absent. The subset of canals present and the extent of their development vary within and among canals and among taxa (Table 1). Furthermore, all species examined have a proliferation of hundreds to thousands of SNs on the head and body, which are described here for the first time. Whole preserved specimens examined using a dissecting microscope with reflected light revealed SNs that appear as small, white, domed structures that are morphologically distinct from the small and broadly distributed complex photophores (light producing organs) found in these fishes (Marranzino, 2016). Neuromast counts are given for one side of the head and body (e.g. in lateral view) unless otherwise noted. Specimen condition was the determining factor in defining the number and distribution of SNs.

CRANIAL LATERAL LINE CANALS

Examination of whole preserved specimens revealed lateral line canal pores in the skin, but could not reveal the degree of ossification of the canals, which are located beneath the skin. In contrast, µCT imaging with 3D reconstruction revealed the degree of ossification of the canals (completely ossified canal with bony pores or incompletely ossified canal with parallel canal walls forming a bony trough; Fig. 4E, F), but could not provide data on canal enclosure by soft tissue. Analysis of histological material provided confirmation of details of canal morphology, enclosure of canals by soft tissue or ossified bone, and neuromast morphology. These methods were used to assess the morphology of the cranial lateral line canals [e.g. supraorbital (SO), preopercular (PO), mandibular (MD) infraorbital (IO) and the canals near the posterior margin of the skull – the otic (OT), post-otic (PT) and supratemporal commissure (ST)] in 28 species.

With the exception of *Cyclothone* spp. in which all cranial lateral line canals are absent, all of the species examined demonstrate variation in the degree to which

the canals are enclosed and ossified (Table 1). Canals are either fully ossified (indicated by the presence of bony canal pores, Stage 4, Bird & Webb, 2014), partially ossified (canal walls represented by a bony trough, which may or may not be covered by a soft tissue canal roof, Stage 2 and 3, respectively) or are absent (Stage 1). The most distinctive feature of the cranial skeleton is the presence of one or two longitudinal ridges extending from each of the frontal bones, which vary morphologically among genera (Fig. 3).

Family Sternoptychidae

The cranial bones in the four species of *Argyropelecus* examined are quite thin and some appear to have a reticulate structure. They also have a prominent bony ridge running longitudinally along each frontal bone (Fig. 1A, C). The ridge starts rostral to the orbit, and becomes more medial, so that between the orbits, the left and right longitudinal ridges nearly touch. Caudal to the orbits, the ridges are more lateral at their posterior end.

The SO, PO and MD canals are present in four species of *Argyropelecus* (*A. hemigymnus*, *A. aculeatus* Valenciennes, 1850, *A. affinis* Garman, 1899, *A. lychnus* Garman, 1899) as revealed in cleared and stained material, histology, µCT images and via examination of whole preserved specimens. Cleared and stained specimens and µCT images show no evidence of bony canal pores that would suggest the presence of completely ossified
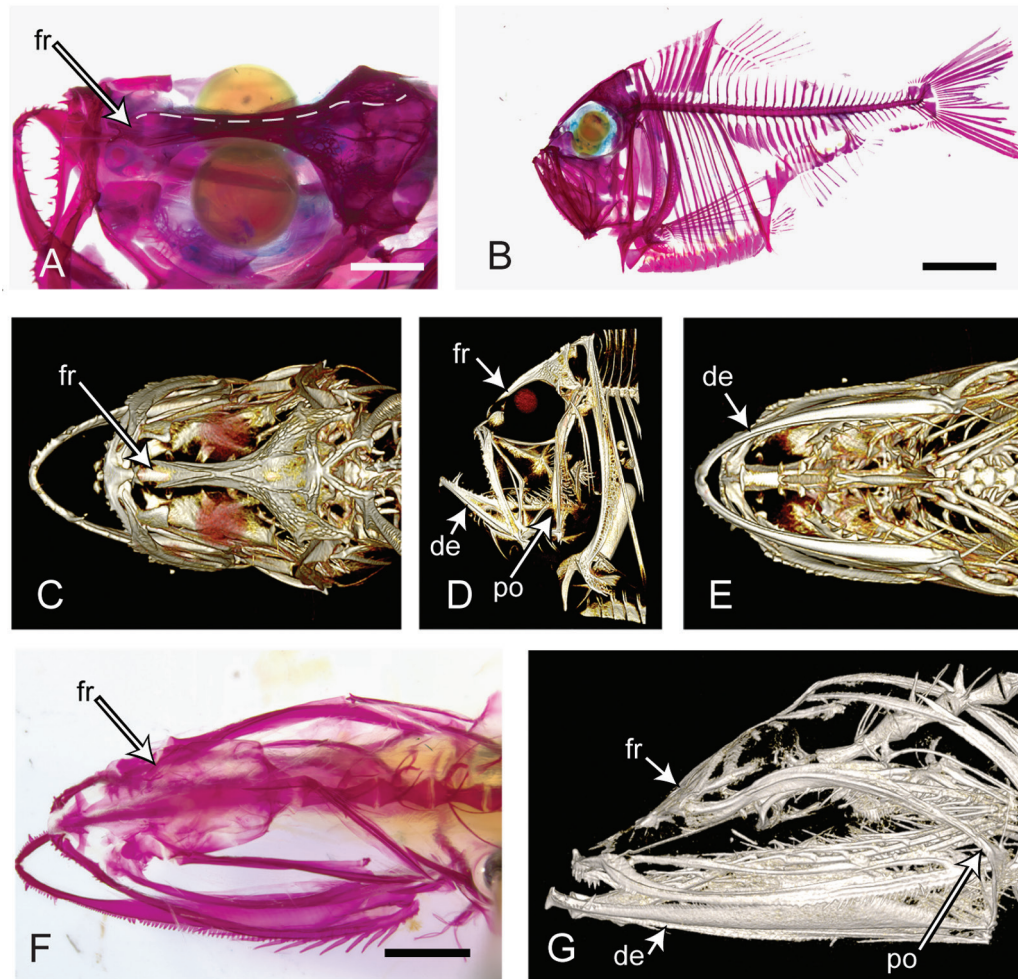

Figure 1. Cranial osteology of *Argyropelecus* and *Cyclothone*. A, B, cleared and stained *A. lychnus* (26-mm SL) in dorsolateral and lateral views showing longitudinal bony ridge extending from frontal bone (white dashed line). C–E, 3D µCT reconstructions of *A. aculeatus* (MCZ 137835, 41-mm SL) in dorsal, lateral and ventral views, respectively, showing elongated troughs in the frontal, dentary and preoperculum. F, *C. acclinidens* (20-mm SL). G, *C. microdon* (MCZ 89489, 50-mm SL). Ossified lateral line canals are absent in both species. fr, frontal, de, dentary, po, preoperculum. Scale bars = (A) 1 mm, (B) 5 mm, (F) 1 mm. C–F, © President and Fellows of Harvard College.

canals. However, bony troughs in the preoperculum and along the mandible indicate the presence of partially ossified PO and MD canals, respectively (Fig. 1B, D, E). The skin covering the PO and MD canals is very thin and often damaged, making the interpretation of canal morphology difficult, but histological analyses of three specimens of *A. aculeatus* confirmed the presence of incompletely ossified SO, PO and MD canals (Table 1). Infraorbital bones and an infraorbital (IO) canal are both absent.

The SO canal is in close association with the longitudinal bony ridge in the frontal bone in all four species of *Argyropelecus* examined. This feature was studied in detail in *A. aculeatus* (Figs 2, 3B). Each ridge starts rostral to the orbit, extends caudally and medially, so that the left and right longitudinal ridges nearly touch between the orbits. Caudal to the orbits, the ridges are situated laterally before terminating (Fig. 2). The SO canal starts rostral to the orbit and medial to the bony ridge. The first SO neuromast is found in the skin overlying the frontal bone (Fig. 2). The next SO canal neuromast is enclosed only by soft tissue. The left and right canals merge into a single canal medial to the orbits, between the ridges, and the left and right canal neuromasts are found within a single median canal. Caudal to the orbits, the two SO canals are separate and SO

canal neuromasts are found within the left and right SO canals. Each SO canal extends laterally passing through the bony ridge as a short ossified canal containing a neuromast. The canal opens to the surface, and the next neuromast (a SO canal neuromast homologue, given its similarity in size to enclosed canal neuromasts) is found on the skin surface (Fig. 2).

In *A. aculeatus*, the MD canal is only partially ossified, appearing as a trough containing two canal neuromasts covered by a thin epithelium. The PO canal originates just caudal to the posterior end of the MD canal and varies in morphology along its length. The first PO neuromast sits in a fully ossified canal below a preopercular spine, but the portion of the PO canal oriented dorso-ventrally is a narrow trough enclosed by a thin epithelium and contains three neuromasts.

Histological analysis showed that canal neuromasts are present in the SO, PO and MD canals of *A. aculeatus*. The neuromasts varied in size among and within canals and with body size, but all appear to be elliptical or diamond shaped with a major axis parallel to the axis of the canal (Marranzino, 2016). In whole specimens, the canal neuromasts appear as opaque, white, oval structures sitting in bony troughs (visible only if the epithelium covering the trough was absent);
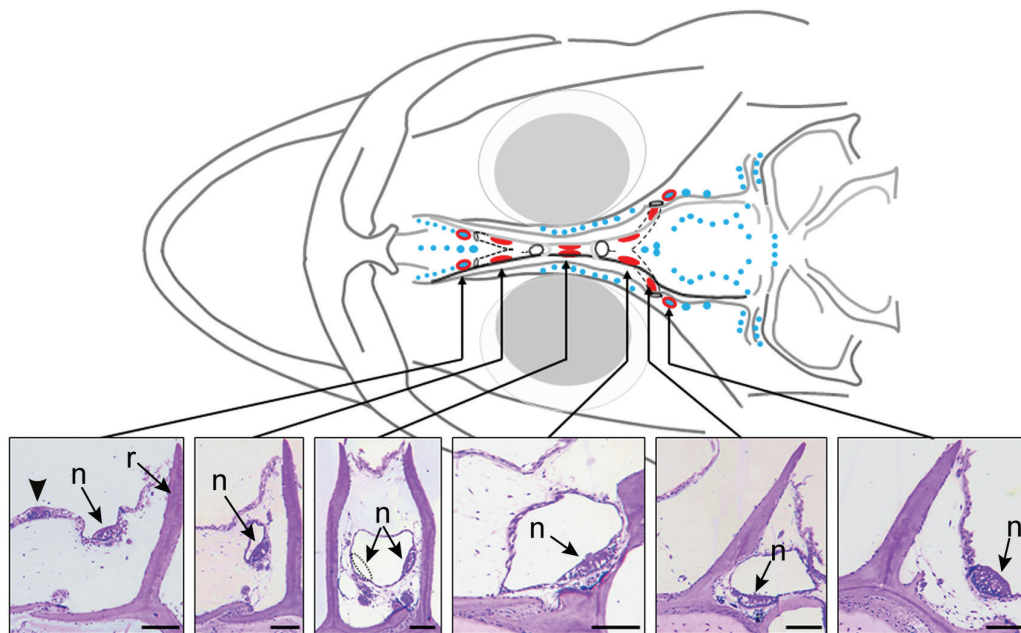

Figure 2. Supraorbital canal and canal neuromasts in *Argyropelecus aculeatus*. Line drawing (in dorsal view) based on a 3D μCT reconstruction (MCZ 137835, 41-mm SL). Canal neuromast and superficial neuromast (SN) distributions based on histological analysis (*n* = 3) and examination of whole specimens (*n* = 11). SNs (blue), canal neuromasts (red), canal neuromast homologues on the skin surface (blue circles with red outline), canal boundaries (black dotted lines) and canal pores (black open circles). Representative transverse histological sections (MCZ 159086, 39-mm SL) show supraorbital canal neuromasts (n) in rostro-caudal sequence (left-to-right images), with the canal extending laterally through the bony ridge (r). In left-most section, arrowhead indicates a SN. In third section from left, dotted line indicates location of the left canal neuromast, which is out of the plane of section. Scale bar = 100 μm. © President and Fellows of Harvard College.
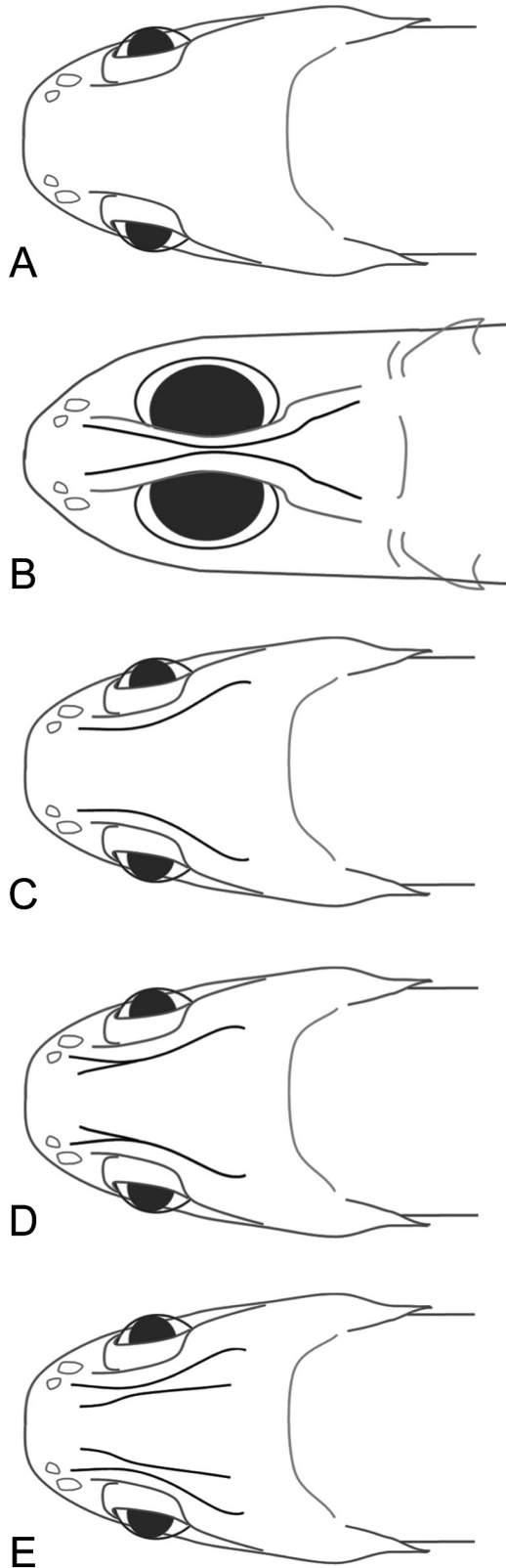
Figure 3. Longitudinal bony ridges on the dorsal surface of head in representative stomiiform genera. Ridges

their locations were confirmed in histological material. Neuromasts are present in troughs in the preopercular and anguloarticular bones in whole preserved *A. hemigymnus*.

Family Gonostomatidae

Examination of whole preserved *Gonostoma elongatum* Gunther, 1878 revealed enclosed lateral line canals. Thin, needle-like bones and partially ossified canals were revealed in µCT reconstructions, and a fully ossified canal was also present in the supracleithrum (Table 1). A bifurcated bony longitudinal ridge is found in the frontal bone rostral to the orbit, which merges into a single ridge at the level of the anterior edge of the orbit (Fig. 3D). The enclosed, but partially ossified SO canal starts rostral to the orbit at the level of the anterior naris and medial to the longitudinal ridge. Caudal to the orbit, epithelial canal pores are found lateral to the ridge suggesting that the canal extends laterally through it. The presence of a trough in the preoperculum and epithelial canal pores in the opercular region indicates that the PO canal is enclosed, but only partially ossified. Epithelial canal pores are not present in the mandible indicating the absence of an MD canal. Three epithelial canal pores ventral to the orbit suggest the presence of an IO canal, but IO bones could not be resolved in µCT images suggesting that the IO canal is unossified or weakly ossified. Epithelial canal pores at the posterior margin of the skull indicate the presence of OT, PT and ST canals, which appear to be incompletely ossified based on µCT data and a fully ossified canal is present in the supracleithrum.

Cleared and stained specimens of *Cyclothone* (*C. acclinidens* Garman, 1899, *C. alba* Brauer, 1906, *C. pseudopallida* Mukhacheva, 1964, *C. signata* Garman, 1899) and µCT reconstruction of *C. microdon* (Gunter,

are bilaterally symmetrical (here, in dorsal view), but are described with reference to the ridge(s) on one side of the head. A, ridge absent in *Cyclothone*, *Bathophilus*, *Malacosteus* and *Neonesthes*. B, one longitudinal ridge extends dorsally from the frontal bone. The longitudinal ridge extends medially, meeting the ridge on the other side of the head medial to the orbits without fusing, in *Argyropelecus* and *Ichthyococcus*. C, one longitudinal ridge is present, but does not meet with or fuse with the ridge on the other side of the head in *Aristostomias*, *Idiacanthus*, *Flagellostomias*, *Pachystomias* and *Tactostoma*. D, one longitudinal ridge is present in the frontal bone, but bifurcates rostral to the orbit, in *Gonostoma*, *Echiostoma* and *Eustomias*. E, two longitudinal bony ridges extend from the frontal bone, but they never meet or fuse with the ridges on the other side of the head in *Astronesthes* and *Opostomias*.

1878) revealed thin, needle-like cranial bones. In contrast to *Gonostoma* and other stomiiforms (see below), all lateral line canals (and troughs indicating the presence of partially ossified canals) are absent, and there is no evidence of a bony longitudinal ridge on the dorsal surface of the frontal bone (Figs 1F, G, 3A; Table 1). Examination of whole preserved specimens (*C. acclinidens*, *C. alba*, *C. braueri* Jespersen and Taning, 1926, *C. microdon*, *C. parapallida* Badcock, 1982, *C. pallida* Brauer, 1902, *C. pseudopallida*, *C. signata*) showed no evidence of epithelial canal pores that would suggest the presence of incompletely ossified canals. Histology (*C. microdon*) confirmed the absence of either soft tissue canals or ossified cranial lateral line canals.

Family Phosichthyidae

Ichthyococcus ovatus (Cocco, 1838) has broad, flat bones (unlike the needle-like bones in other taxa) that are quite thin and difficult to differentiate from soft tissue in μCT reconstructions. Both fully and partially ossified lateral line canals are present (Table 1). Canal pores are absent in the frontal bone, but a longitudinal bony ridge is present (Fig. 3B) suggesting that an enclosed, but partially ossified, SO canal is present (similar to *Argyropelecus*). The PO canal is ossified with one prominent bony pore ventrally, but in lateral view, μCT cannot resolve the canal, so it was interpreted as being weakly ossified or only partially ossified. A trough in what appears to be the dentary bone was interpreted as an incompletely ossified MD canal.

Family Stomiidae

Canal morphology in representatives of 13 stomiid genera showed considerable variation among taxa. Examination of three whole preserved *Astronesthes niger* Richardson, 1845, one *A. niger* prepared histologically and three μCT reconstructions of *A. gemmifer* Goode & Bean, 1896 revealed both epithelial canal pores and bony pores, indicating the presence of enclosed and fully ossified SO, PO, MD and IO canals, as well as canals extending caudally from the SO canal (probably OT, PT and ST canals; Table 1). Two longitudinal ridges (inner, outer) extend dorsally from each frontal bone, but never fuse into a single ridge, or meet medially (Fig. 3E). The SO canal begins near the nares, medial to the two bony ridges, and then caudal to the orbit it passes through the outer longitudinal ridge so that it is lateral to both ridges at the canal's posterior end. Histological material (*A. niger*) confirmed that the SO canal is fully ossified and that SO canal neuromasts vary in diameter (78–128 μm, $n = 3$). Epithelial canal pores are present in the skin of *A. niger* at the posterior margin of the skull indicating the presence of one or more canals caudal to the SO canal (the OT, PT and/or ST canals). These canals appear to be enclosed and are either partially or fully ossified, but only some of the canals could be resolved in μCT reconstructions. Bony and epithelial canal pores are visible on the ventral (horizontal) arm of the preoperculum indicating the presence of an enclosed and fully ossified PO canal. The MD canal has an unusually high number of bony and epithelial canal pores and appears to be fully ossified rostrally, but is partially ossified caudally (represented by a trough). A single epithelial canal pore is found ventral to the orbit in whole preserved specimens, indicating the presence of an incompletely ossified IO canal. This was confirmed in histological material (*A. niger*) in which one IO neuromast (~80 μm in diameter) was observed, but the IO canal could not be resolved in μCT reconstructions of *A. gemmifer*.

Examination of one whole preserved *Echiostoma barbatum* Lowe, 1843 and μCT reconstructions of three other specimens revealed the presence of epithelial and bony canal pores, respectively (Table 1). The cranial bones are thin, making them difficult to visualize in μCT reconstructions. Two longitudinal bony ridges (inner, outer) are present in the frontal bone rostral to the orbit and merge into a single ridge medial to the orbits (Fig. 3E). The SO canal begins medial to the ridges at the level of the nares and extends laterally through the bony ridges caudal to the orbit. The SO canal appears to be partially ossified (a trough is present), but is fully enclosed (indicated by the presence of epithelial canal pores) more caudally. A bony trough and epithelial canal pores indicate the presence of fully enclosed and partially ossified canals caudal to the SO canal (probably OT, PT and ST canals). The PO canal appears to be fully ossified in the ventral portion of the preoperculum, but is enclosed and only partially ossified in the dorsal portion of the canal. Bony and epithelial pores along the mandible indicate that the MD canal is enclosed and fully ossified rostrally, and enclosed but incompletely ossified caudally (appearing as a trough, Fig. 4F). IO bones could not be resolved in μCT reconstructions, and IO epithelial pores were not visible, indicating the absence of an IO canal.

A μCT reconstruction of one *Aristostomias tittmanni* Welsh, 1923 revealed SO, MD and PO canals (Table 1; Figs 4A–E, 5A). A single bony longitudinal ridge is present (Fig. 3C). The SO canal begins rostral to the orbit as a partially ossified canal (a trough in the nasal bone) and is fully ossified medial to the longitudinal ridge. Caudal to the orbit the SO canal extends laterally through the ridge. The canal is narrow, but the canal pores appear to be relatively large compared to those in other taxa (Fig. 4B). A fully ossified PO canal in the form of a hollow tube with pores at either end is found in the preoperculum. An MD canal is indicated by the presence of bony pores in the rostral portion of the mandible and a trough is found more caudally (Fig. 4E) indicating only partial
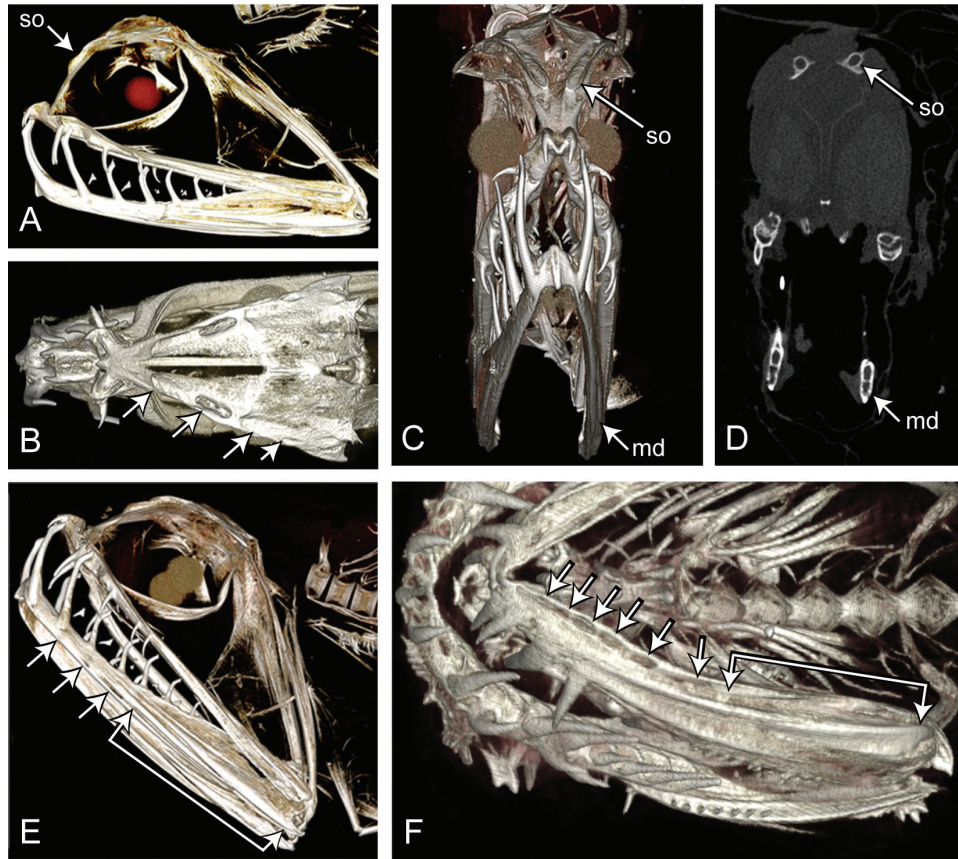
Figure 4. 3D reconstructions of μCT data revealing cranial osteology of representative stomiids showing fully and partially ossified lateral line canals. See text for additional descriptions. A–E, *Aristostomias tittmanni* (MCZ 163949, 156-mm SL) in lateral (A), dorsal (B), rostral (C) and ventro-lateral (E) views and in a 2D section (D) showing the supraorbital (so) and mandibular (md) canals. F, *Echiostoma barbatum* (MCZ 148298) in ventral view, indicating the location of fully ossified rostral portion of the MD canal with pores, and a partially ossified segments portion of the mandibular canal more caudally. Arrows indicate canal pores; arrow bracket indicates elongated canal troughs. © President and Fellows of Harvard College.

ossification. Neither IO bones nor bony pores were visible in the posterior region of the skull in μCT images, indicating the absence of these canals.

Two μCT reconstructions of *Malacosteus niger* Ayres, 1848 and *Malacosteus* sp. revealed several canals that were difficult to differentiate from the surrounding soft tissue (Table 1; Fig. 5D). The SO canal is fully ossified, but μCT 3D reconstructions show that a longitudinal bony ridge is absent (Fig. 3A). Troughs in the preoperculum and in the rostral portion of the dentary indicate the presence of partially ossified PO and MD canals, respectively (Fig. 5D). Neither IO bones nor bony pores in the posterior region of the skull were visible indicating the absence of these canals.

Two μCT reconstructions of *Neonesthes capensis* (Gilchrist & von Bonde, 1924) and *Neonesthes* sp. revealed both fully and partially ossified canals, which are narrow with relatively large bony pores, similar to those in *Aristostomias* (Table 1; Fig. 5B). A

longitudinal bony ridge in the frontal bone is absent (Fig. 3A). Bony pores in the frontal and preopercular bones indicate the presence of fully ossified SO and PO canals, respectively. A μCT reconstruction reveals that the MD canal is well ossified rostrally, but is incompletely ossified more caudally, appearing as a trough in the bone. Infraorbital bones could not be resolved in μCT images suggesting the absence of an IO canal. Bony pores and a trough in the bone located caudal to the SO canal suggest the presence of fully and partially ossified canals, respectively, at the posterior margin of the skull.

Three μCT reconstructions of *Pachystomias* sp. revealed well-ossified narrow canals with small canal pores (Table 1, Fig. 5C). A longitudinal bony ridge extends dorsally along the length of the frontal bone (Fig. 3C). The SO canal starts rostral to the orbit and medial to the bony ridge as an incompletely ossified canal, which is fully ossified rostral to the orbit, but
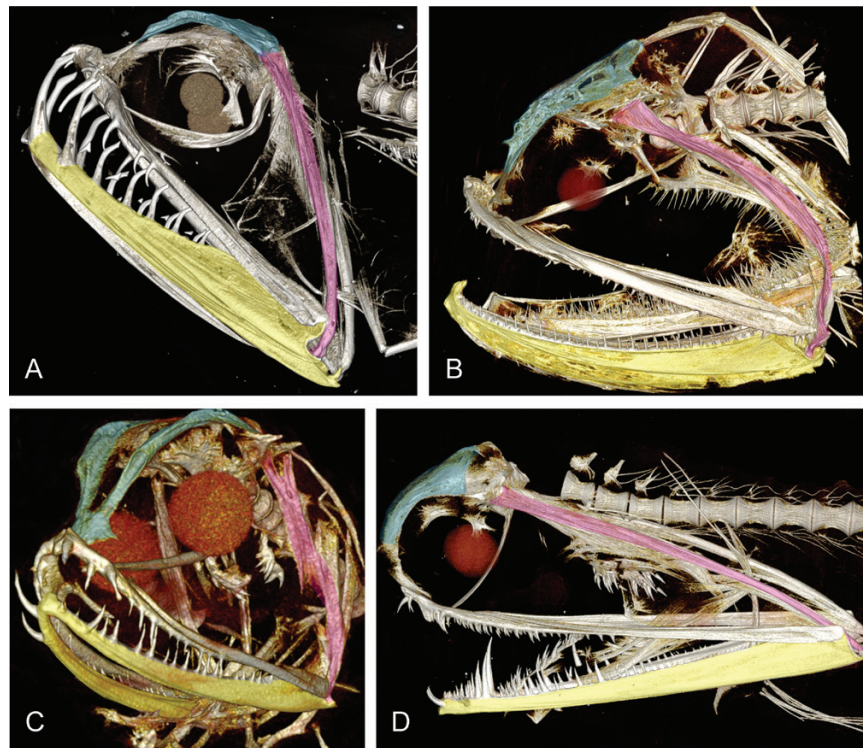
Figure 5. 3D reconstructions of µCT data revealing cranial osteology of selected stomiiforms. The supraorbital canal (in the frontal bone, blue), preopercular canal (in the preopercular bone, pink) and mandibular canal (in the dentary and angu-loarticular bones, yellow) in (A) *Aristostomias tittmanni* (MCZ 163949, 156-mm SL), (B) *Neonesthes capensis* (MCZ 132802, 147-mm SL), (C) *Pachystomias* sp. and (D) *Malacosteus niger* (MZ 131758, 110-mm SL). Note: specimen condition (affected by collection, fixation and long-term storage) has a substantial effect on the resolution in µCT reconstructions. It is not clear if incompletely ossified canals or bones that are not visible in µCT renderings, for instance, are due to bone damage, degradation in fixation and storage or inability to resolve thin bones in µCT images. © President and Fellows of Harvard College.

remains medial to the bony ridge along its entire length. The PO canal is fully ossified ventrally, but only partially ossified dorsally (represented by a trough). A trough in the mandible indicates the presence of an incompletely ossified MD canal. Infraorbital bones could not be resolved in µCT images. An ossified canal with two pores is visible caudal to the termination of the SO canal indicating the presence of another canal (Fig. 5C).

A µCT reconstruction of *Rhadinesthes decimus* (Zugmayer, 1911) revealed thin cranial bones that could not be easily differentiated from surrounding soft tissue. However, 2D cross-sections (as in *A. tittmanni*, Fig. 4D) indicate the presence of several cranial canals (Table 1). The SO canal appears to be fully ossified, but a longitudinal bony ridge is not present. The PO canal is fully ossified ventrally, but appears to be only partially ossified more dorsally. A fully ossified MD canal is present, but IO, PT, ST or OT canals could not be visualized.

Canal pores in the skin of a whole preserved *Bathophilus filifer* (Garman, 1899) indicate the

presence of SO, PO and MD canals that are enclosed and either partially or fully ossified. An enclosed SO canal starts rostral to the orbit but a longitudinal bony ridge is not present (Fig. 3A). Epithelial canal pores indicate the presence of a canal caudal to the SO canal (probably the OT canal). Epithelial canal pores are visible in the opercular region and on the mandible, indicating the presence of fully enclosed PO and MD canals, respectively. Epithelial canal pores are not present ventral to the orbit suggesting the absence of an IO canal.

Examination of one whole preserved *Eustomias hulleyi* Gomon & Gibbs, 1985 revealed small epithelial pores indicating the presence of several canals (Table 1). A longitudinal bony ridge in the frontal bone bifurcates rostral to the orbit, but merges into a single ridge at the level of the orbit (Fig. 3D). An enclosed SO canal is present at the level of the posterior naris, medial to the bifurcated longitudinal ridge and appears to extend laterally through the ridge, terminating caudal to the orbit. An epithelial canal pore caudal to the SO canal suggests the presence of another canal at the

posterior margin of the skull (probably the OT canal). Epithelial canal pores are found in the opercular region and on the mandible indicating the presence of enclosed PO and MD canals, respectively. Epithelial canal pores are not present ventral to the orbit suggesting the absence of an IO canal.

One whole preserved *Flagellostomias boureei* (Zugmayer, 1913) was studied and revealed epithelial canal pores indicating the presence of several enclosed canals (Table 1). A single bony longitudinal ridge extends dorsally from the frontal bone (Fig. 3C). The SO canal appears to remain medial to the longitudinal ridge along its entire length. Epithelial canal pores caudal to the end of the SO canal suggest the presence of the OT canal. Epithelial canal pores are visible in the opercular region and the rostral portion of the mandible, indicating the presence of enclosed PO and MD canals, respectively. Two canal pores in the epithelium rostral and ventral to the orbit, suggest the presence of an IO canal.

Two whole preserved *Idiacanthus antrostomus* Gilbert, 1890 have small epithelial canal pores on the head suggesting the presence of enclosed cranial canals that are either partially or fully ossified (Table 1). A longitudinal bony ridge extends dorsally from the frontal bone (Figs 3C, 8C). The SO canal begins at the level of the posterior naris, medial to the bony ridge, extends lateral to the bony ridge, and terminates caudal to the orbit. Smaller epithelial canal pores appear to be associated with a canal at the posterior margin of the head, probably the OT canal. Pores are not visible in the opercular region, suggesting the absence of a PO canal. Epithelial canal pores in the rostral portion of the mandible and ventral to the orbit indicate the presence of enclosed MD and IO canals, respectively.

Examination of one whole preserved *Opostomias micripnus* (Günther, 1878) revealed the presence of epithelial canal pores (Table 1). Two longitudinal bony ridges (inner and outer) extend dorsally from the frontal bone and extending caudal to the orbit, but they are not fused (Fig. 3E). The fully enclosed SO canal begins rostral to the orbit, sitting medial to both the inner and outer bony ridges. The canal then extends laterally through the inner bony ridge and then through the outer bony ridge, and is found lateral to both ridges before terminating. The SO canal terminates caudal to the orbit. Epithelial canal pores are found caudal to the posterior end of the SO canal indicating the presence of enclosed canals, probably the OT, PT and ST canals. Epithelial canal pores in the opercular region indicate the presence of an enclosed PO canal. A large number of epithelial canal pores along the mandible and three pores ventral to the orbit indicate the presence of enclosed MD and IO canals, respectively.

The study of one whole preserved *Tactostoma macropus* Bolin, 1939 revealed a single longitudinal bony ridge extending dorsally from the frontal bone (Fig. 3C).

The SO canal originates rostral to the anterior naris and medial to the bony ridge and extends laterally through the bony ridge caudal to the orbit. Caudal to the posterior-most SO canal pore, epithelial canal pores indicate the presence of what is probably the OT canal, which appears to be partially ossified. Epithelial canal pores in the opercular region indicate the presence of an enclosed PO canal. A large number of MD pores (ten) are present, extending halfway along the length of the mandible, but the canal continues caudally as an open trough. Two epithelial canal pores rostral and ventral to the orbit indicate the presence of an enclosed IO canal.

SUPERFICIAL NEUROMAST DISTRIBUTIONS

A proliferation of hundreds to thousands of small, round, white, domed structures is found on the head and trunk in *A. hemigymnus*, in other species of *Argyropelecus* and in representatives of four other genera of Stomiiformes (Table 2). These structures were initially observed in whole preserved specimens and their identity as SNs was confirmed with SEM (based on the presence of a kinocilium and multiple stereocilia on the apical surface of each hair cell) and transverse histological sections (showing typical arrangement of hair cell nuclei and more basal support cell nuclei). SN proliferations were indicated in an additional six stomiid genera, for a total of 17 species representing 11 genera in three of the four families of stomiiform fishes. These small SNs are morphologically distinct from the small, complex photophores (light producing organs) that are broadly distributed in these fishes (Marranzino, 2016).

Family Sternoptychidae

Hundreds of small, round, white, domed structures (~50–100 μm in diameter) were found on the head and body of four species of *Argyropelecus* (Table 2; Fig. 6). These are densely placed, with six to eight per millimetre in linear series. They were also found on the caudal fin (*A. hemigymnus*; Fig. 6C) and pectoral fins (*A. aculeatus*). Histology (*A. aculeatus*; Fig. 7C, D) and SEM (in *A. hemigymnus*; Fig. 7F, G) confirmed that these structures are SNs (Fig. 7). SEM revealed linear series of oval neuromasts with a longer axis parallel to the line in which they are situated. The sensory hair cells have very long kinocilia and are restricted to an area in the centre of each neuromast (Fig. 7G). Hair cell orientation is defined by the location of the kinocilium relative to the multiple stereocilia on the surface of each hair cell. Hair cell orientation determines the axis of best physiological sensitivity of the neuromast, which in this case is perpendicular to the line of neuromasts (parallel with the rosto-caudal axis of the fish). Histological analysis of a portion of the head

Table 2. Number of superficial neuromasts in stomiiforms (this study) and other teleosts (as reported in the literature)

Order and family	Species	Size (mm SL)	Number of SNs
Stomiiformes			
Sternoptychidae	*Argyropelecus aculeatus*	30–41.5	~356
	A. affinis	49	~420
	A. hemigymnus	30–36.5	~521
	A. lychnus	29	~220
Gonostomatidae	*Cyclothone microdon*	52–60	~533
	Gonostoma elongatum	50	~1111
Stomiidae	*Idiacanthus antrostomus*	79	~2200
	Tactostoma macropus	84	~2286
Characiformes			
Characidae*	*Astyanax mexicanus* (blind)	45.3	2647
	Astyanax mexicanus (eyed)	55.2	2900
	Gymnocorymbus ternetzi	20.8–26.4	2471
	Hasemania nana	21.1	485
	Hyphessobrycon herbertaxelrodi	20.4–21.9	1477
	H. megalopterus	24.9–26.8	1565
	Inpaichthys kerri	25.9–28.4	467
	Paracheirodon innesi	12.8	787
Beloniformes			
Zenarchopteridae†	*Zenarchopterus dunckeri*	84.1	1449
Perciformes			
Apogonidae‡	*Fowleria variegate*	49.6	2403
	Ostorhinchus doederleini	60.6	4088
Gobiidae§,‖	*Glossogobius olivaceus*	82	4828
	Pterogobius elapoides	68	1068
Odontobutidae‖	*Odontobutis obscura*	72	1598
Rhyacicthyidae¶	*Rhyacichthys aspro*	47.3	308

Neuromast counts in stomiiforms are conservative estimates for one side of head and body in whole preserved specimens.
*Sumi et al. (2015).
†Hirota et al. (2015).
‡Sato et al. (2017).
§Asaoka, Nakae & Sasaki (2010).
‖Asaoka, Nakae & Sasaki (2012).
¶Asaoka, Nakae & Sasaki (2014).

(*A. aculeatus*; 39-mm standard length, SL) revealed hundreds of SNs (Fig. 6B, 7C, D). An examination of whole preserved specimens revealed that all four species of *Argyropelecus* demonstrated a similar proliferation and distribution of SNs, with ~220 SNs in one *A. lychnus*, and ~420 SNs in one *A. affinis* (Fig. 6A) . Variability in specimen condition resulted in notable variation in the number of SNs observed. Comparison of SN number and distributions in multiple specimens of the same species revealed as many as ~356 SNs on one side of the head and body of *A. aculeatus* (Fig. 6B) and as many as ~521 SNs on one side of the head and body of *A. hemigymnus* (Fig. 6C; Table 2).

Family Gonostomatidae
Hundreds of small, round, white, domed structures (~30–40 μm in diameter) were interpreted to be SNs

and stand out against the darkly pigmented skin of the head and elongated trunk of *G. elongatum* (Fig. 8B, D). They occur on the head and in vertical lines that run around the circumference of the trunk between large photophores in each body segment. In a small individual (50-mm SL), ~500 SNs are present on one side of the head and more than 500 are present on one side of the trunk. In some cases, SNs are located between depressions in a linear series (Fig. 8E), supporting the interpretation that the depressions are actually the locations of SNs that had been damaged and lost. Accounting for these missing SNs, it is likely that there are more than 1200 SNs on one side of the body in one specimen of *G. elongatum*.

Examination of specimens of five species of *Cyclothone* that had an intact epidermis (*C. acclinidens*, *C. braueri*, *C. microdon*, *C. pseudopallida*, *C. signata*), revealed numerous, small, round, domed
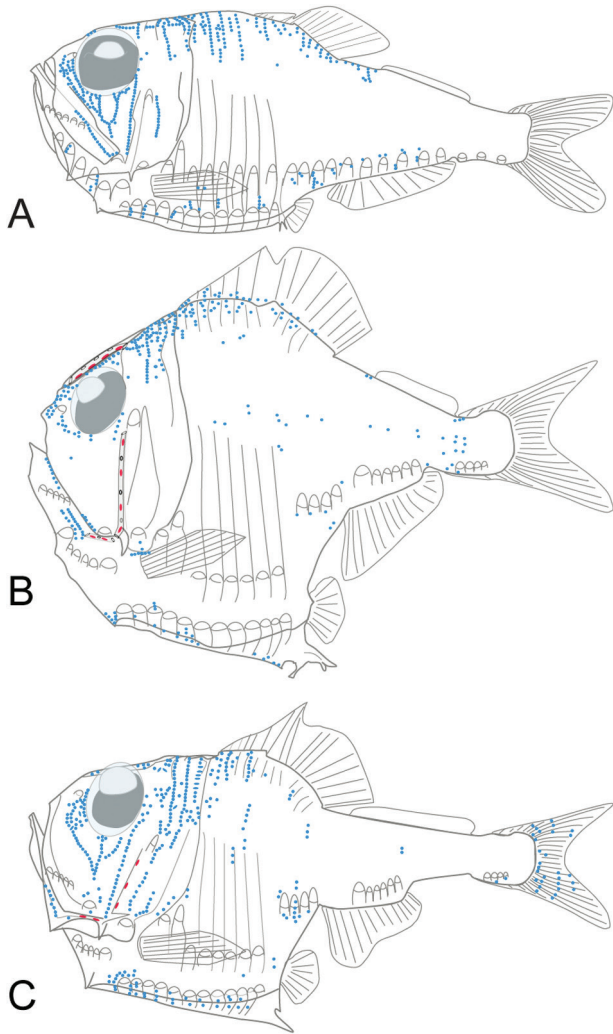
Figure 6. Superficial neuromast distribution in *Argyropelecus* spp. Distribution of SNs in (A) *A. affinis*, (B) *A. aculeatus* (based on 11 fish) and (C) *A. hemigymnus* (based on five fish), drawn from whole preserved specimens. Outlines from Baird (1971). Blue, superficial neuromasts; red, canal neuromasts. Neuromasts are enlarged to enhance visibility.

structures (SNs; ~55–80 μm in diameter) on the head and trunk. They are found in lines and clusters in similar locations on the head and trunk and on the pectoral, pelvic and caudal fins (Fig. 8A) in all species. Histology (*C. microdon*) confirmed their identity as SNs, but SEM (*C. signata*) revealed only a few SNs in which the sensory hair cells could be visualized. An examination of four whole preserved *C. microdon* revealed several hundred SNs on one side of the head and trunk in a single specimen. Due to variation in specimen condition, a more complete assessment of neuromast distribution

was obtained by studying several specimens of *C. microdon*, which revealed more than 530 SNs on one side of the head and trunk (Table 2).

Family Stomiidae

Well-preserved specimens of representative stomiids had SNs appearing as numerous small, white, domed structures (30–40 μm in diameter) arranged in lines that stand out against the darkly pigmented skin of the head and trunk (Fig. 8G).

Acknowledging the damage to the epidermis on the head and body, it was determined that ~214 SNs are present on the head and more than 2000 SNs are present on the elongated trunk (Fig. 8C, G) of a specimen of *I. antrostomus*. An assessment of the number and distribution of SNs and small depressions on the skin (see above) provides a conservative estimate of well over 2000 SNs on one side of the head and trunk. A similar number and distribution of SNs was found in a specimen of *T. macropus*, with ~450 SNs on the head and over 1840 SNs in discrete vertical lines running around the circumference of the trunk, with one line of neuromasts per body segment. Additional SNs were found on the dorsal and ventral surfaces of the trunk and SNs form horizontal lines between the vertical lines found on each body segment (not counted). Thus, a conservative estimate suggests that this specimen of *T. macropus* has ~2286 SNs on one side of the head and trunk (Table 2).

Specimens of other stomiids (*A. niger*, *B. filifer*, *E. barbatum*, *E. hulleyi*, *F. boureei* and *O. micripnus*) had a damaged epidermis with no evidence of the small, white, domed structures seen in other taxa. However, numerous small depressions were observed on the head and in discrete vertical lines around the circumference of their body (one per body segment, between serial photophores; Fig. 8F) as in *Gonostoma*, *Idiacanthus* and *Tactostoma*. Histological analysis of one *A. niger* confirmed the presence of numerous, closely placed SNs in vertical lines on the head (Fig. 8H, I). These SNs are smaller than canal neuromasts and morphologically distinct from photophores, which are convex and rise above the surrounding epithelium (Fig. 8F). They are densely placed in vertical lines (with as many as 13 in a single vertical row) in the same locations as depressions observed in whole preserved specimens of *A. niger* (and in other stomiids). This confirms the interpretation that the small depressions in the skin are the locations of SNs that were damaged and lost.

DISCUSSION

This study has shown that the lateral line system of the stomiiform fishes is characterized by partially or
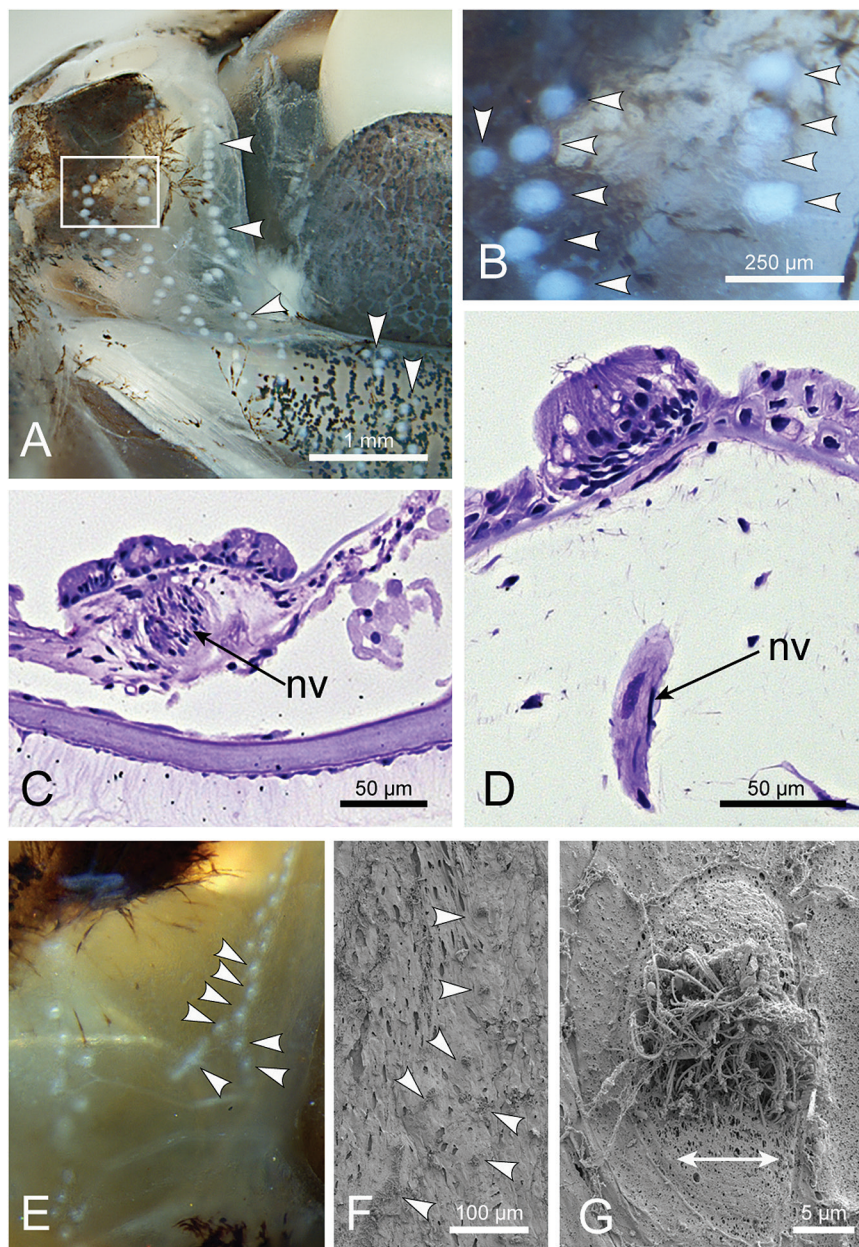
Figure 7. Superficial neuromasts (SNs) in *Argyropelecus* spp. A, SNs (arrowheads) rostral to the eye of *A. affinis* (49-mm SL), see also Figure 6A. B, close-up of SNs (arrowheads) from box in (A), rostral to the eye. C, histological section showing closely placed SNs with nerve innervation (nv) in *A. aculeatus* on dorsal midline of head. D, close-up of an SN in same general location as (C), showing nerve (nv) innervating SN. E, area rostral to eye in *A. hemigymnus* (MCZ 150985, 30-mm SL) with lines of closely placed SNs (arrowheads); see also Figure 6C. F, SEM of the same portion of the specimen as in (H) indicating the same SNs (arrowheads). G, close-up of a representative SN (from F) reveals an oval outline with the population of hair cells (with long kinocilia) located in a central, circular area; axis of best physiological sensitivity of the neuromast is rostro-caudal (perpendicular to the line of neuromasts; double-headed arrow). C–G, © President and Fellows of Harvard College.

completely reduced cranial lateral line canals, which are accompanied by proliferations of hundreds to thousands of small SNs on the head and trunk.

Cyclothone lacks all of the cranial lateral line canals, but representatives of all of the other stomiiform genera examined have a mixture of fully ossified
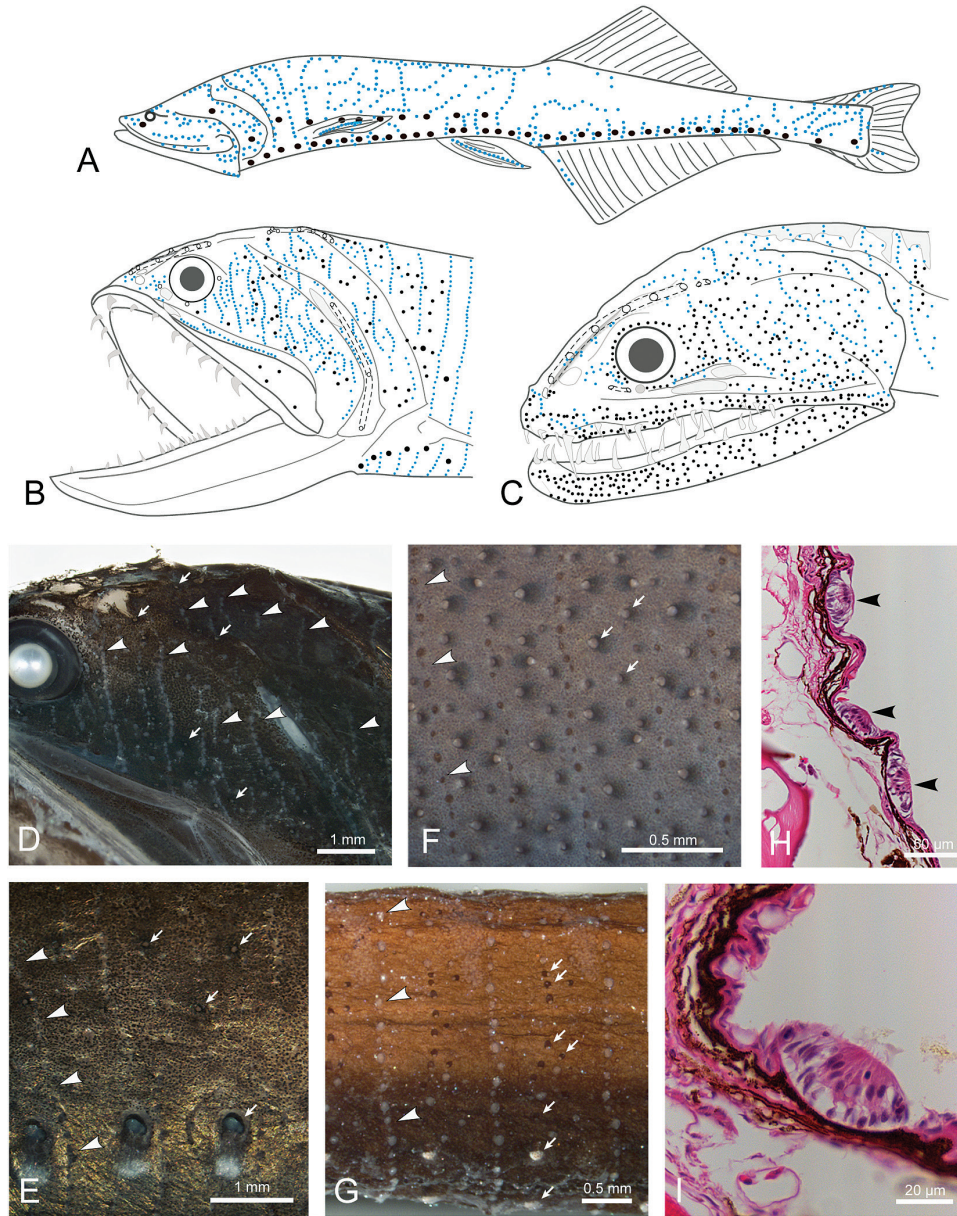
Figure 8. Superficial neuromasts (SNs) in representative gonostomatids and stomiids. SN distribution in (A) *Cyclothone* spp. (based on whole preserved specimens of *C. acclinidens*, *C. braueri*, *C. microdon*, *C. signata*, body outline from Mukhacheva, 1966), (B) *Gonostoma elongatum* (50-mm SL; canals based on several whole preserved specimens, 50- to 100-mm SL), (C) *Idiacanthus antrostomus* (79-mm SL; canals based on two whole preserved specimens, 41 and 79-mm SL). Blue – SNs, black – small, complex photophores, open circles – pores and dotted lines – canals. Grey – location of simple photophores. D, *Gonostoma elongatum* (50-mm SL; rostral to left) with small, white, domed structures (SNs, arrowheads) densely placed in vertical lines that contrast with pigmented epithelium. Small arrows – photophores. E, several body segments [lateral view; boundary defined by vertical line of depressions (arrowheads)] on trunk of *G. elongatum* (50-mm SL) showing discrete vertical lines of small depressions (locations of damaged SNs) between lines of photophores (small arrows). F, several body segments in lateral view [body segment boundaries defined by vertical lines of depressions, the locations of damaged SNs (arrowheads)] on the trunk of *Bathophilus filifer* (46-mm SL) between lines of comparably sized photophores. G, several body segments (in latero-ventral view), bounded by vertical lines of small SNs (arrowheads) on trunk of *I. antrostomus* (79-mm SL; rostral to left) between lines of photophores (small arrows). H, histological section of head of *Astronesthes niger* (MCZ 52847, 52-mm SL; haematoxylin and eosin stained) showing multiple SNs (arrowheads) over pigment layer. I, close-up of SN in *A. niger* showing apical sensory hair cell nuclei, more basal support cell nuclei and underlying pigment layer. H, I, © President and Fellows of Harvard College.

canals and/or partially ossified canals (represented by bony troughs) that may be enclosed by soft tissue. Together with the osteological data available for representatives of 20 other stomiiform genera (Weitzman, 1967, 1974; Fink, 1985; Marranzino, 2016; this study; Table 1), it is suggested that reduced cranial lateral line canals may be a general feature of the order Stomiiformes. However, different canals appear to have been reduced or lost among families and among genera within those families. For instance, among stomiids, the PO canal is absent in *Idiacanthus*, but the IO canal is absent in *Bathophilus*, *Echiostoma* and *Eustomias*. Among the Sternoptychidae, the IO canal is absent in *Argyropelecus*, but this was the only genus examined. Among the Gonostomatidae, only the MD canal is absent in *Gonostoma*, but all the canals are absent in *Cyclothone*. In addition, the number and position of the longitudinal ridges found in the frontal bone, and through which the ossified SO canal passes, also vary among stomiiform taxa (Fig. 3). Particular ridge phenotypes occur among genera in different stomiiform families. Ridges are absent in *Cyclothone* (Gonostomatidae) and in *Bathophilus*, *Malacosteus* and *Neonesthes* (Stomiidae); the ridge on each side of the head meets medial to the eyes in *Argyropelecus* (Sternoptychidae) and *Ichthyococcus* (Phosichthyidae); and a ridge that bifurcates rostrally occurs in *Gonostoma* (Gonostomatidae) as well as in *Echiostoma* and *Eustomias* (Stomiidae). The other two ridge morphologies were only observed in stomiid genera. The phylogenetic relationships among genera could reveal evolutionary patterns in canal loss and ridge morphology. However, while phylogenetic relationships among stomiid genera have been hypothesized (Fink, 1985; Near *et al.*, 2013; Kenaley, Devaney & Fjeran, 2014; Davis, Sparks & Smith, 2016), the taxon sampling in those studies do not allow any conclusions to be drawn about the evolution of canal or longitudinal ridge morphology among genera examined in this study.

Contrary to Handrick (1901), this study has shown that *A. hemigymnus*, as well as other species of *Argyropelecus* and other stomiiforms, have a proliferation of hundreds to thousands of SNs that rival the SN proliferations in other fishes (Table 2). This feature of the lateral line system may be a synapomorphy uniting certain stomiiform clades or the entire order, but a test of these hypotheses will require detailed morphological analyses of additional stomiiform taxa and of hypothesized stomiiform sister taxa, whose identification is somewhat controversial. The Osmeriformes + Retropinnidae (Near *et al.*, 2012), Osmeriformes (Betancur-R *et al.*, 2013; Davis *et al.*, 2016; Smith *et al.*, 2016) and Osmeridae (Near *et al.*, 2013) have all been hypothesized to be the sister group of the Stomiiformes. Smith *et al.* (2016) placed

the Glaxiiformes as the sister group of Stomiiformes + Osmeriformes. Betancur-R *et al.* (2013) identified a clade containing Argentiniformes, Salmoniformes, Esociformes and Galaxiiformes as the sister group to the clade containing the Stomiiformes. In other studies, Argentiniformes (Davis *et al.*, 2016) and a clade containing the Argentiniformes, Salmoniformes and Esociformes (Near *et al.*, 2012, 2013; Smith *et al.*, 2016) were hypothesized to be the sister group to the clade that includes the Stomiiformes + Neoteleostei.

The lateral line system in most of these taxa is not well known, but the distribution of neuromasts in salmonids (*Oncorhynchus*, *Salmo*; Disler, 1971; Jollie, 1984; Montgomery *et al.*, 2003; Cech & Mussen, 2006) may be informative. Salmonids have well-ossified, narrow lateral line canals and a relatively small number of SNs located in lines rostral to the olfactory organ, on the preoperculum and in the otic/post-otic region (Disler, 1971; Jollie, 1984; Cech & Mussen, 2006), which are reminiscent of those in *Amia calva* (Allis, 1889) and in cichlids (Peters, 1973; Becker *et al.*, 2016). However, each of the cranial lateral line canals contains a relatively high number of small neuromasts (Disler, 1971; Jollie, 1984) compared with those in other teleosts (e.g. zebrafish, *Danio rerio*, Webb & Shirey, 2003; cichlids, Peters, 1973; Tarby & Webb, 2003). For instance, more than 12 neuromasts are in the infraorbital (circumorbital) canal series in *Salmo* (Jollie, 1984) and more than 100 neuromasts are found in the trunk canal (Disler, 1971), which is more than twice that typically found in these canals in most other teleosts. Disler (1971) reported that the number of neuromasts in the canal series on the head of salmonids continues to increase through the larval period and that secondary neuromasts ('secondary accessory hillocks') bud off from the primary neuromasts on the trunk. This process, which results in the formation of 'stitches', i.e. dense lines of SNs with the same hair cell orientation, has also been documented in zebrafish and other fishes (Ghysen, Wada & Dambly-Chaudiere, 2014). Thus, if the process of canal formation were truncated in a salmonid (resulting in paedomorphic 'reduced canals', Webb, 1989), a relatively large number of small presumptive canal neuromasts would be left on the skin. A proliferation (via budding) of these neuromasts and of the other SNs on the head and trunk could result in the sorts of neuromast numbers and distributions described here among stomiiform fishes (a peramorphic feature). Interestingly, the small size of neuromasts in adult stomiiforms is similar to that of the larvae of other fishes (*Amia*, Allis, 1889; *Danio rerio*, Webb & Shirey, 2003; cichlids, Bird & Webb, 2014; Webb *et al.*, 2014), suggesting that stomiiform neuromasts are paedomorphic features of these fishes. Other paedomorphic features noted among deep-sea fishes, include the morphology of the eyes, swimbladder, kidney, skin and muscles (Marshall, 1984). Detailed comparative developmental studies are needed to explicitly test the hypothesis that the evolution of the lateral line

system of stomiiform fishes is the outcome of dissociated heterochrony resulting in a combination of paedomorphic and peramorphic features (see Webb *et al.*, 2014; Bird & Webb, 2014).

The functional significance of variation in lateral line system morphology among stomiiform taxa could be revealed by looking at ecological correlates, but these are difficult to discern based on the data in this study for several reasons. (1) All *Cyclothone* species lack lateral line canals on the head and trunk despite interspecific differences in geographical distribution, depth ranges, presence/absence of diel migration, observed posture (vertical, horizontal), reproductive strategy (sexual dimorphism, hermaphroditism) and feeding habits (Froese & Pauly, 2017). Furthermore, *Cyclothone microdon* is the only species in the genus for which SN number has been assessed (~533 SNs on the head and body), so an evaluation of ecological correlates will require additional data. (2) The complement of canals present does not vary among the four species of *Argyropelecus* studied, but they demonstrate considerable variation in SN number (~220 to ~521). For instance, *A. lychnus*, which has the lowest number of SNs, has the shallowest reported depth range (200–700 m), but while the species with higher numbers of SNs are known to make excursions into the bathypelagic (to more than 2000–3800 m), they are typically found at mesopelagic depths like those inhabited by *A. lychnus* (Froese & Pauly, 2017). Several species of *Argyropelecus* are noted to feed at dusk and somewhat selectively (*A. aculeatus*) or more opportunistically (*A. hemigymnus*, Froese & Pauly, 2017), but additional data on feeding preferences and migratory habits are needed to assess ecological variation and establish ecological correlates. (3) Representative species of three stomiid genera (*Gonostoma*, *Idiacanthus*, *Tactostoma*) have ~1100 to ~2286 SNs on the head and elongate body and all demonstrate diel vertical migration, but variation in SN numbers do not correlate with what is known about depth ranges, migratory habits or reproductive strategies (sexual dimorphism, hermaphroditism; Froese & Pauly, 2017). (4) Finally, ecological correlates of lateral line morphology among stomiiform families are confounded by the fact that SN numbers tend to be correlated with body form. For instance, the sternoptychids have a short, deepened, laterally compressed body with SNs that tend to occur in vertical lines on the dorsal half of the head and trunk. In *Cyclothone* (Gonostomatidae), which lacks all canals, the body is elongate and canals are absent, but SNs are scattered over the head and body, with some indication of segmental organization on the trunk. In *G. elongatum* (Gonostomatidae) and in all of the stomiid species examined, SNs are found in lines on the head and in segmental vertical lines on the elongate body.

In the absence of meaningful ecological correlates, the occurrence of relatively high numbers of SNs in the Stomiiformes and in other diverse deep-sea taxa [e.g. Saccopharyngiformes, Aulopiformes, Myctophiformes, Gadiformes (Macrouridae), Lophiiformes, Notocanthiformes, Stephanoberyciformes; Marshall, 1954, 1979; Marshall & Staiger, 1975; Marshall, 1996; Harold, 2002] suggests that SN proliferation is an adaptation for detecting water disturbances in the light-limited environment of the deep sea. In a general sense, the broad distribution of SNs on the head and body presumably provides high sensitivity to hydrodynamic disturbances in the relatively quiet waters of the deep sea. The combination of reduced lateral line canals [which leaves SNs (= canal neuromast homologues) on the skin surface] and the proliferation of these and other SNs increase the relative number of neuromasts functioning as velocimeters (SNs) as opposed to those functioning as accelerometers (canal neuromasts). Based solely on neuromast number, this represents a shift in the relative importance of these two mechanosensory submodalities compared with shallow water fishes, which tend to have well-developed canals accompanied by a relatively small number of SNs (reviewed in Coombs, Janssen & Webb, 1988; Webb, 2014b). By enhancing the detection of the velocity component of short-range hydrodynamic disturbances, these animals are probably more sensitive to stimuli generated by mid-water predators, prey and/or potential mates, especially in the absence of high levels of ambient hydrodynamic noise. The distribution of vertical and horizontal lines of SNs on the head and trunk makes it likely that fish are sensitive to flow stimuli originating in a variety of directions. However, the rostro-caudal orientation of the hair cells of SNs in vertical lines on the head (e.g. in *Argyropelecus*) and the occurrence of vertical lines of superficial SNs on the trunk of other genera suggest a bias for detection of water flows parallel to the rostro-caudal axis of the body. A more thorough assessment of hair cell orientation in the SNs within and among lines or regions on the head and trunk will be required to interpret and model the functional attributes of these sensory receptor arrays. Such data will not only have interesting implications for our understanding of their sensory ecology, but for the design of artificial sensor arrays for underwater vehicles.

Direct observations of the behaviour of live stomiiform fishes will contribute to functional interpretations of lateral line morphology. *In situ* video observations reveal that some stomiiforms spend time suspended fairly motionless in the water column [Monterey Bay Aquarium Research Institute (MBARI) videos D144, 2010; D442, 2012]. This behaviour may reduce metabolic demands as well as self-generated water flows, thereby allowing fish to more effectively detect

short-range hydrodynamic disturbances generated by other organisms in the water column. With integration of inputs from other sensory systems (e.g. vision), the lateral line system may play a role in initiating directed prey strikes, such as those documented in *Argyropelecus* and *Chauliodus* (Merrett & Roe, 1974; MBARI video D551, 2013). The adaptive significance of SN proliferation for prey detection, in particular, is supported by experimental work on the surface and cave forms of the Mexican blind cavefish, *A. mexicanus* (e.g. Yamamoto & Jeffery, 2011). SNs may also mediate responses to hydrodynamic cues arising from potential mates in the context of reproductive behaviour (e.g. Butler & Maruska, 2016). This would be advantageous in the deep sea where population densities are low and finding a mate is a significant challenge. Tests of these hypotheses will require *in situ* behavioural studies.

Finally, we have demonstrated that specimen condition is critical for an assessment of SN morphology and distribution in stomiiform fishes; even those specimens that appeared to be in excellent condition upon first examination had some skin damage when studied in more detail. We conclude that Handrick's (1901) report of only a small number of SNs in *A. hemigymnus* was the result of poor specimen condition and that the high numbers of SNs on the head and trunk reported in this study are fairly conservative. The ongoing development of novel net materials and technologies that reduce damage during collection (Childress *et al.*, 1978), continued sampling of intact specimens that are carefully preserved, and additional high resolution video documentation of behaviour *in situ* will reveal more about the role of the lateral line system in the sensory biology and behaviour of these deep-sea fishes.

ACKNOWLEDGEMENTS

REFERENCES

Allis EPJ. 1889. The anatomy and development of the lateral line system in *Amia calva*. *Journal of Morphology* **2:** 463–542 + plates.

Asaoka R, Nakae M, Sasaki K. 2010. Description and innervation of the lateral line system in two gobioids, *Odontobutis obscura* and *Pterogobius elapoides* (Teleostei: Perciformes). *Ichthyological Research* **58:** 51–61.

Asaoka R, Nakae M, Sasaki K. 2012. The innervation and adaptive significance of extensively distributed neuromasts in *Glossogobius olivaceus* (Perciformes: Gobiidae). *Ichthyological Research* **59:** 143–150.

Asaoka R, Nakae M, Sasaki K. 2014. Innervation of the lateral line system in *Rhyacichthys aspro*: the origin of superficial neuromast rows in gobioids (Perciformes: Rhyacichthyidae). *Ichthyological Research* **61:** 49–58.

Baird RC. 1971. The systematics, distribution, and zoogeography of the marine hatchetfishes (family Sternoptychidae). *Bulletin of the Museum of Comparative Zoology* **142:** 115–123.

Becker EA, Bird NC, Webb JF. 2016. Post-embryonic development of canal and superficial neuromasts and the generation of two cranial lateral line phenotypes. *Journal of Morphology* **277**: 1273–1291.

Betancur-R R, Broughton RE, Wiley EO, Carpenter K, Lopez JA. Li C, Holcroft NI, Arcila D, Sanciangco M, Cureton JC II. 2013. The tree of life and a new classification of bony fishes. *PLoS Currents* **5**. doi: 10.1371/currents. tol.53ba26640df0ccaee75 bb165c8c26288.

Bigelow HB, Cohen DM, Dick MM, Gibbs RH Jr, Grey M, Morrow JE Jr, Schultz LP, Walters V. 1964. *Fishes of the Western North Atlantic*, Part 4. New Haven: Sears Foundation for Marine Research, 599.

Bird NC, Webb JF. 2014. Heterochrony, modularity, and the functional evolution of the mechanosensory lateral line canal system of fishes. *EvoDevo* **5:** 21.

Butler JM, Maruska KP. 2016. Mechanosensory signaling as a potential mode of communication during social interactions in fishes. *The Journal of Experimental Biology* **219:** 2781–2789.

Caruso C. 1989. Systematics and distribution of the Atlantic chaunacid anglerfishes (Pisces: Lophiiformes). *Copeia* **1:** 153–165.

Cech J Jr, Mussen T. 2006. *Determining how fish detect fish screens and testing potential fish screen enhancements*. California Energy Commission, PIER Energy-Related Environmental Research Program. CEC-500-2006-117.

Childress JJ, Barnes AT, Quetin LB, Robison BH. 1978. Thermally protecting cod ends for the recovery of living deep-sea animals. *Deep-Sea Research* **25:** 419–422.

Coombs S, Janssen J, Webb JF. 1988. Diversity of lateral line systems: phylogenetic, and functional considerations. In:

Atema J, Fay RR, Popper AN, Tavolga WN, eds. *Sensory biology of aquatic animals*. New York: Springer, 553–593.

Davis MP, Holcroft NI, Wiley EO, Sparks JS, Leo Smith W. 2014. Species-specific bioluminescence facilitates speciation in the deep sea. *Marine Biology* **161:** 1139–1148.

Davis MP, Sparks JS, Smith WL. 2016. Repeated and widespread evolution of bioluminescence in marine fishes. *PLoS ONE* **11**. doi: 10.1371/journal.pone.0155154

De Busserolles F, Marshall NJ, Collin SP. 2014. The eyes of lanternfishes (Myctophidae, Teleostei): novel ocular specializations for vision in dim light. *The Journal of Comparative Neurology* **522:** 1618–1640.

Denton EJ, Gray JAB. 1989. Some observations on the forces acting on the neuromasts in fish lateral line canals. In: Coombs S, Görner P, Münz H, eds. *The mechanosensory lateral line: neurobiology and evolution*. New York: Springer, 229–246.

Disler NN. 1971. *Lateral line sense organs and their importance in fish behavior*. Jerusalem: Israel Program for Scientific Translations (from Russian), 328.

Douglas RH, Partridge JC. 2011. Vision: visual adaptations to the deep sea. In: Farrell AP, ed. *Encyclopedia of fish physiology, Vol. 1*. San Diego: Academic Press, 166–182.

Fange R, Larsson A, Lidman U. 1972. Fluids and jellies of the acusticolateralis system in relation to body fluids in *Coryphaenoides rupestris* and other fishes. *Marine Biology* **17:** 180–185.

Fink WL. 1985. Phylogenetic interrelationships of the stomiid fishes (Teleostei: Stomiiformes). *Miscellaneous Publications of the Museum of Zoology*, University of Michigan No. 171.

Froese R, Pauly D, eds. 2017. FishBase, Version (02/2017). Available at: www.fishbase.org (accessed June 2017).

Gagnon YL, Sutton TT, Johnsen S. 2013. Visual acuity in pelagic fishes and mollusks. *Vision Research* **92:** 1–9.

Ghysen A, Wada H, Dambly-Chaudiere C. 2014. Patterning the posterior lateral line in teleosts: evolution of development. In: Bleckmann H, Mogdans J, eds. *Flow sensing in air and water – behavioural, neural and engineering principles of operation*. Berlin: Springer, 295–318.

Hall BK. 1986. The role of movement and tissue interactions in the development and growth of bone and secondary cartilage in the clavicle of the embryonic chick. *Journal of Embryology and Experimental Morphology* **93:** 133–152.

Handrick K. 1901. Nervensystems und der leuchtorgane von *Argyropelecus hemigymnus*. *Zoologica* **32:** 1–69.

Harold AS. 2002. Order Stomiiformes. In: Carpenter K, ed. *The living marine resources of the Western Central Atlantic, Vol. 2: bony fishes part 1 (Acipenseridae to Grammatidae)*. UN Food and Agriculture Organization, 881–913.

Hirota K, Asaoka R, Nakae M, Sasaki K. 2015. The lateral line system and its innervation in *Zenarchopterus dunckeri* (Beloniformes: Exocoetoidei: Zenarchopteridae): an example of adaptation to surface feeding in fishes. *Ichthyological Research* **62:** 286–292.

Jakubowski M. 1974. Structure of the lateral-line canal system and related bones in the berycoid fish *Hoplostethus mediterraneus* Cuv. et Val. (Trachichthyidae, Pisces). *Acta Anatomica* **87:** 261–274.

Jollie M. 1984. Development of the head skeleton and pectoral girdle of salmons, with a note on the scales. *Canadian Journal of Zoology* **62:** 1757–1778.

Kenaley CP, Devaney SC, Fjeran TT. 2014. The complex evolutionary history of seeing red: molecular phylogeny and the evolution of an adaptive visual system in deep-sea dragonfishes (Stomiiformes: Stomiidae). *Evolution* **68:** 996–1013.

Lawry JV Jr. 1972a. A presumed near field pressure receptor in the snout of the lantern fish, *Tarletonbeania crenularis* (Myctophidae). *Marine Behaviour and Physiology* **1:** 295–303.

Lawry JV Jr. 1972b. The trigeminofacial innervation of the cephalic lateral line organs and photophores of the lantern fish *Tarletonbeania crenularis* (Myctophidae). *Marine Behaviour and Physiology* **1:** 285–293.

Marranzino AN. 2016. *Flow sensing in the deep sea: morphology of the lateral line system in stomiiform fishes.* M.S. Thesis, University of Rhode Island. Open Access Master's Theses Paper 889. Available at: http://digitalcommons.uri.edu/theses/889

Marshall NB. 1954. *Aspects of deep-sea biology*. London: Hutchinson.

Marshall NB. 1965. Systematic and biological studies of the Macrourid fishes (Anacanthini-Teleostii). *Deep-Sea Research* **12**: 299–322.

Marshall NB. 1979. *Developments in deep-sea biology*. Poole: Blandford Press.

Marshall NB. 1984. Progenetic tendencies in deep-sea fishes. In: Potts GW, Wootton RJ, eds. *Fish reproduction*. London: Academic Press, 91–100.

Marshall NJ. 1996. The lateral line systems of three deep-sea fish. *Journal of Fish Biology* **49:** 239–258.

Marshall NB, Staiger JC. 1975. Aspects of structure, relationships and biology of deep-sea fish *Ipnops murrayi* (family Bathypteroidae). *Bulletin of Marine Science* **25:** 101–111.

Maynard SD. 1982. *Aspects of the biology of mesopelagic fishes of the genus Cyclothone (Pisces: Gonostomatidae) in Hawaiian waters*. Ph.D. Dissertation, University of Hawaii, 514.

McHenry MJ, Liao JC. 2014. The hydrodynamics of flow stimuli. In: Coombs S, Bleckmann H, Fay RR, Popper AN, eds. *The lateral line system*. New York: Springer, 73–98.

Mead G, Rubinoff I. 1966. *Avocettinops yanoi*, a new nemichthyid eel from the Southern Indian Ocean. *Breviora* **241:** 1–6.

Merrett NR, Roe HSJ. 1974. Patterns and selectivity in the feeding of certain mesopelagic fishes. *Marine Biology* **28:** 115–126.

Montgomery J, Bleckmann H, Coombs S. 2014. Sensory ecology and neuroethology of the lateral line. In: Coombs S, Bleckmann H, Fay RR, Popper AN, eds. *The lateral line system*. New York: Springer, 121–149.

Montgomery JC, McDonald F, Baker CF, Carton AG, Ling N. 2003. Sensory integration in the hydrodynamic world of rainbow trout. *Proceedings of the Royal Society of London B: Biological Sciences* **270:** S195–S197.

Moore J. 1993. Phylogeny of the Trachichthyiformes (Teleostei: Percomorpha). *Bulletin of Marine Sciences* **1:** 114–136.

Mukhacheva VA. 1966. The composition of species of the genus *Cyclothone* (Pisces, Gonostomatidae) in the Pacific

Ocean. In: Rass TS, ed. *Fishes of the Pacific and Indian Oceans biology and distribution, Vol. 73*. Jerusalem: Academy of Science Israel Program for Scientific Translation, 98–146.

Near TJ, Dornburg A, Eytan RI, Keck BP, Smith WL, Kuhn KL, Moore JA, Price SA, Burbrink FT, Friedman M, Wainwright PC. 2013. Phylogeny and tempo of diversification in the superradiation of spiny-rayed fishes. *Proceedings of the National Academy of Sciences of the United States of America* **110:** 12738–12743.

Near TJ, Eytan RI, Dornburg A, Kuhn KL, Moore JA, Davis MP, Wainwright PC, Friedman M, Smith WL. 2012. Resolution of ray-finned fish phylogeny and timing of diversification. *Proceedings of the National Academy of Sciences of the United States of America* **109:** 13698–13703.

Nelson JS, Grande TC, Wilson MVH. 2016. *Fishes of the world, 5th edn*. New York: Wiley and Sons.

Nielsen JG, Bertelsen E. 1985. The gulper-eel family Saccopharyngidae (Pisces, Anguilliformes). *Steenstrupia* **11:** 157–206.

Peters HM. 1973. Anatomie und Entwicklungsgeschichte des Laterallissystems von *Tilapia* (Pisces, Cichlidae). *Z Morph der Tiere* **74:** 89–161.

Pothoff T. 1984. Clearing and staining technique. In: Moser HC, ed. *Ontogeny and systematics of fishes, Special Publication No. 1*. Lawrence, KS: American Society of Ichthyologists and Herpetologists, 35–37.

Sato M, Asaoka R., Nakae M, Sasaki K. 2017. The lateral line system and its innervation in *Lateolabrax japonicus* (Percoidei *incertae sedis*) and two apogonids (Apogonidae), with special reference to superficial neuromasts (Teleostei: Percomorpha). *Ichthyological Research* **64:** 308–330.

Schwalbe MAB, Bassett DK, Webb JF. 2012. Feeding in the dark: lateral line mediated feeding behavior in the peacock cichlid, *Aulonocara stuartgranti*. *Journal of Experimental Biology* **215:** 2060–2071.

Smith WL, Stern JH, Girard MG, Davis MP. 2016. Evolution of venomous cartilaginous and ray-finned fishes. *Integrative and Comparative Biology* **56:** 950–961.

Sumi K, Asaoka R, Nakae M, Sasaki K. 2015. Innervation of the lateral line system in the blind cavefish *Astyanax mexicanus* (Characidae) and comparisons with the eyed surface-dwelling form. *Ichthyological Research* **62:** 420–430.

Sutton TT, Hopkins TL. 1996. Trophic ecology of the stomiid (Pisces: Stomiidae) fish assemblage of the eastern Gulf of Mexico: strategies, selectivity and impact of a top mesopelagic predator group. *Marine Biology* **127:** 179–192.

Tarby ML, Webb JF. 2003. Development of the supraorbital and mandibular lateral line canals in the cichlid, *Archocentrus nigrofasciatus*. *Journal of Morphology* **255:** 44–57.

Theisen B. 1959. On the cranial morphology of *Ipnops murrayi* Günther, 1878 with special reference to the relationships between the eyes and the skull. *Galathea Report* **8:** 7–18.

Webb JF. 1989. Neuromast morphology and lateral line trunk canal ontogeny in two species of cichids: An SEM study. *Journal of Morphology* **202:** 53–68.

Webb JF. 2014a. Lateral line morphology and development and implications of the ontogeny of flow sensing in fishes. In: Bleckmann H, Mogdans J, eds. *Flow sensing in air and water – behavioural, neural and engineering principles of operation*. Berlin: Springer, 127–146.

Webb JF. 2014b. Morphological diversity, development, and evolution of the mechanosensory lateral line system. In: Coombs S, Bleckmann H, Fay RR, Popper AN, eds. *The lateral line system*. New York: Springer, 17–72.

Webb JF, Bird NC, Carter L, Dickson J. 2014. Comparative development and evolution of two lateral line phenotypes in lake Malawi cichlids. *Journal of Morphology* **275:** 678–692, cover illustration.

Webb JF, Shirey JE. 2003. Postembryonic development of the cranial lateral line canals and neuromasts in zebrafish. *Developmental Dynamics* **228:** 370–385.

Weitzman SH. 1967. The origin of the stomiatoid fishes with comments on the classification of salmoniform fishes. *Copeia* **1967:** 507–540.

Weitzman SH. 1974. Osteology and evolutionary relationships of the Sternoptychidae, with a new classification of stomiatoid families. *Bulletin of the American Museum of Natural History* **153:** 331–476.

Yamamoto Y, Jeffery WR. 2011. Blind cavefish. In: Farrell AP, ed. *Encyclopedia of fish physiology – from genome to environment*. San Diego: Academic Press.

Yoshizawa M, Goricki S, Soares D, Jeffery WR. 2010. Evolution of a behavioral shift mediated by superficial neuromasts helps cavefish find food in darkness. *Current Biology* **20:** 1631–1636.

APPENDIX 1

Specimens examined. Sources of study material: MCZ, Museum of Comparative Zoology, Harvard University; JFW, uncatalogued specimens in research collection of JF Webb, housed at University of Rhode Island (voucher specimens to be deposited at the MCZ, Harvard). Collection method: IKMT, Isaacs-Kidd mid-water trawl; OCTT, opening/closing Tucker trawl; TTIC, Tucker trawl with thermally insulated cod end; ANM, AN Marranzino. Whole preserved specimens (fixed in 10% formalin, stored in 70% ethanol or 10% formalin) were studied under a dissecting microscope with reflected light, in addition to using these methods: C&S, cleared and stained for bone and cartilage; Hem, haematoxylin staining; Hist, histology (paraffin and/or plastic); SEM, scanning electron microscopy; μCT, micro-computed tomography. See Material and methods for details.

STERNOPTYCHIDAE

Argyropelecus aculeatus: MCZ 159086 [30- to 40.5-mm SL, $n = 9$; Hist (1)]; MCZ 137835 (41-mm SL, $n = 1$, μCT); JFW 1162 [28.5- to 38.0-mm SL, $n = 4$; NW Atlantic; 15 August 2014; *R/V Endeavor*; TTIC; 500 m; coll. N Hobbs, B Seibel; ID'ed by ANM; Hist ($n = 2$), Hem].

Argyropelecus affinis: JFW 041 (41-mm SL, *n* = 1; Catalina Basin, CA; 1988, *R / V New Horizon* CBAT; IKMT; coll. J. Webb; ID'ed ANM; C&S); JFW 2118 (49-mm SL, *n* = 1; East. Cent. Pac., 32° N 120° W; 2010; *R / V New Horizon* CBAT; TTIC; coll. B Seibel; ID'ed by ANM).

Argyropelecus hemigymnus: MCZ 150985 (30- to 35-mm SL, *n* = 5); MCZ 135828 (size unkn., *n* = 5); JFW 042 (22-mm SL, *n* = 1; Catalina Basin, CA; 1988, *R / V New Horizon* CBAT; IKMT; coll. J. Webb; ID'ed ANM; C&S).

Argyropelecus lychnus: JFW 040, 041, 1005 (12.5- to 36-mm SL, *n* = 22; Catalina Basin, CA; 1988; *R / V New Horizon*, CBAT; IKMT; ID'ed by ANM); JFW 1181 (10- to 29-mm SL, *n* = 3; Monterey Bay, CA; 10 September 2014; OCTT; 600 m; coll. S Haddock (gift); ID'ed by ANM).

GONOSTOMATIDAE

Cyclothone acclinidens: JFW 036, 039, 062, 064 [21- to 48-mm SL, *n* = 6, C&S (3); Catalina Basin, CA, 1988, *R / V New Horizon*, CBAT, IKMT; ID'ed by ANM].

Cyclothone alba: JFW 039 (28-mm SL, *n* = 1; Catalina Basin, CA, 1988, *R / V New Horizon* CBAT, IKMT; ID'ed by ANM), JFW 061 (28-mm SL, *n* = 1; NW Atlantic, Brown's Bank, July 1985, SSV *Westward*, W-83; ID'ed by ANM).

Cyclothone braueri: JFW 2119 (28- to 29-mm SL, *n* = 2, SEM, Hem; Eastern Atlantic, 32° N 120° W, 2010, *R / V New Horizon*, TTIC; coll. B Seibel; ID'ed by ANM).

Cyclothone microdon: MCZ 89489 (50-mm SL, *n* = 1; μCT); JFW 1160 [44.5- to 56.5, *n* = 6; Hem (4), Hist (2), SEM (2); NW Atlantic, 15 August 2014, *R / V Endeavor*, TTIC; coll. N Hobbs, B Seibel; ID'ed by ANM].

Cyclothone parapallida: JFW 061 (33.5-mm SL, *n* = 1; Brown's Bank, NW Atlantic, Brown's Bank, July 1985, SSV *Westward*, W-83; ID'ed by ANM; C&S).

Cyclothone pallida: JFW 061 (31.5- to 35-mm SL, *n* = 2; Brown's Bank, NW Atlantic, Brown's Bank, July 1985, SSV *Westward*, W-83; ID'ed by ANM; C&S).

Cyclothone pseudopallida: JFW 051 [22- to 27.5-mm SL, *n* = 2; C&S (1), SEM (1); Catalina Basin, CA, 1988, *R / V New Horizon*, CBAT, IKMT; ID'ed by AN Marranzino]; JFW 061 [26.5- to 27.5-mm SL, *n* = 1; C&S (*n* = 1); NW Atlantic, Brown's Bank, July 1985, SSV *Westward*, W-83; ID'ed by ANM].

Cyclothone signata: JFW 039, 059 (13- to 35-mm SL, *n* = 11; C&S [*n* = 8], Hem [*n* = 1], Hist [*n* = 1], SEM [*n* = 1]; Catalina Basin, CA, 1988, *R / V New Horizon* CBAT, IKMT; ID'ed by ANM).

Gonostoma elongatum: MCZ 140857 (146- to 182, *n* = 2; μCT); JFW 1173, 1176 (50- to 100-mm SL, *n* = 6; NW Atlantic, 16–17 August 2014, *R / V Endeavor*; TTIC; coll. N Hobbs, B Seibel; ID'ed by ANM).

PHOSICHTHYIDAE

Ichthyococcus ovatus: MCZ 47693 (51.8-mm SL, *n* = 3; μCT).

STOMIIDAE

Aristostomias tittmanni: MCZ 163949 (156-mm SL, *n* = 1, μCT); MCZ 149494 (77-mm SL, *n* = 1, μCT).

Astronesthes niger: MCZ 98847 (25- to 45-mm SL, *n* = 3), MCZ 52847 [52, *n* = 1, Hist (*n* = 1)].

Astronesthes gemmifer: MCZ 133451 (146-mm SL, *n* = 1, μCT); MCZ 42864 (121-mm SL, *n* = 1, μCT), MCZ 148312 (163-mm SL, *n* = 1, μCT).

Bathophilus filifer: JFW 2131 [46-mm SL, *n* = 1, Hist and SEM (*n* = 1); Pacific, 2010, *R / V New Horizon*, TTIC, 900 m; coll B. Seibel; ID'ed by ANM].

Echiostoma barbatum: MCZ 148298 (187- to 248-mm SL, *n* = 3, μCT); JFW 2115 (210-mm SL, *n* = 1, Northwestern Atlantic, 37°46.142N, 71°11.702W, September 2011; *R / V Endeavor*; 650 m TTIC; coll B. Seibel; ID'ed by ANM).

Eustomias hulleyi: MCZ 100873 (118-mm SL, *n* = 1).

Flagellostomias boureei: JFW 2109 (79-mm SL, *n* = 1, Hawaii, 5 June 2012; 500 m TTIC; coll. A. Bockus; ID'ed by A. Bockus).

Idiacanthus antrostomus: JFW 1182 (79-mm SL, *n* = 1; Monterey Bay, CA, 20 September 2014, OCTT, 600 m, coll. S. Haddock; ID'ed by ANM); JFW 2106 (41-mm SL, *n* = 1; Gulf of CA, July 2015, TTIC; coll. B. Seibel; ID'ed by ANM).

Malacosteus niger: MCZ 131758 (110-mm SL, *n* = 1, μCT).

Malacosteus sp.: MCZ 131758, 110-mm SL (*n* = 2, μCT).

Neonesthes capensis: MCZ 132802 (147-mm SL, *n* = 1, μCT).

Neonesthes sp.: MCZ 132800, 138-mm SL (*n* = 1, μCT).

Opostomias micripnus: MCZ 132634 (270-mm SL, *n* = 1).

Pachystomias sp.: Specimen data unavailable (*n* = 3, μCT).

Rhadinesthes decimus: MCZ 64832, 242-mm SL (*n* = 1, μCT).

Tactostoma macropus: JFW 1183 (84-mm SL, *n* = 1, Monterey Bay, CA, 20 September 2014, OCTT, 600 m; coll. S. Haddock; ID'ed by ANM).